Calhoun: The NPS Institutional Archive

DSpace Repository

Reports and Technical Reports | All Technical Reports Collection

1989-05

Sea surface temperature fields derived from aircraft and ship observations during FASINEX 1986

Lind, Richard J.; Shaw, William J.

Monterey, California. Naval Postgraduate School

https://hdl.handle.net/10945/29079

This publication is a work of the U.S. Government as defined in Title 17, United States Code, Section 101. Copyright protection is not available for this work in the United States.

Downloaded from NPS Archive: Calhoun

http://www.nps.edu/library

Calhoun is the Naval Postgraduate School's public access digital repository for research materials and institutional publications created by the NPS community. Calhoun is named for Professor of Mathematics Guy K. Calhoun, NPS's first appointed -- and published -- scholarly author.

Dudley Knox Library / Naval Postgraduate School
411 Dyer Road / 1 University Circle
Monterey, California USA 93943

NPS-63-89-001

NAVAL POSTGRADUATE SCHOOL

Monterey, California

SEA SURFACE TEMPERATURE FIELDS DERIVED FROM AIRCRAFT AND SHIP OBSERVATIONS DURING FASINEX 1986

Richard J. Lind

William J. Shaw

May 1989

FASINEX Contribution No. 72

Approved for public release; distribution is unlimited.

Prepared for: National Science Foundation
Washington, DC 20550

FedDocs
D 208.14/2
NPS-63-89-001

DUDLEY KNOX LIBRARY
NAVAL POSTGRADUATE SCHOOL
MONTEREY CALIFORNIA 93943

Fo 41
L 58.

NAVAL POSTGRADUATE SCHOOL
Monterey, California 93943

Rear Admiral R. Austin
Superintendent

J. M. Shull
Provost

The work reported herein was supported in part by the National Science Foundation (Ocean Sciences) with funds provided by Grant OCE-86-03050.

Reproduction of all or part of the report is authorized.

This report was prepared by:

Department of Meteorology

Dean of Science and Engineering

UNCLASSIFIED

URITY CLASSIFICATION OF THIS PAGE

REPORT DOCUMENTATION PAGE

REPORT SECURITY CLASSIFICATION UNCLASSIFIED	1b RESTRICTIVE MARKINGS
SECURITY CLASSIFICATION AUTHORITY	3 DISTRIBUTION / AVAILABILITY OF REPORT Approved for public release; distribution is unlimited.
DECLASSIFICATION / DOWNGRADING SCHEDULE	
ERFORMING ORGANIZATION REPORT NUMBER(S) NPS-63-89-001	5 MONITORING ORGANIZATION REPORT NUMBER(S)
NAME OF PERFORMING ORGANIZATION Naval Postgraduate School 6b OFFICE SYMBOL (If applicable) 63	7a NAME OF MONITORING ORGANIZATION
ADDRESS (City, State, and ZIP Code) Monterey, CA 93943-5000	7b ADDRESS (City, State, and ZIP Code)
NAME OF FUNDING / SPONSORING ORGANIZATION ational Science Foundation 8b OFFICE SYMBOL (If applicable)	9 PROCUREMENT INSTRUMENT IDENTIFICATION NUMBER NSF Grant OCE-86-03050
ADDRESS (City, State, and ZIP Code) Washington, DC 20550	10 SOURCE OF FUNDING NUMBERS PROGRAM ELEMENT NO / PROJECT NO / TASK NO / WORK UNIT ACCESSION NO

TITLE (Include Security Classification)
SEA SURFACE TEMPERATURE FIELDS DERIVED FROM AIRCRAFT AND SHIP OBSERVATIONS DURING FASINEX 1986 (U)

PERSONAL AUTHOR(S) Richard J. Lind and William J. Shaw

TYPE OF REPORT	13b TIME COVERED	14 DATE OF REPORT (Year, Month, Day)	15 PAGE COUNT
Interim	FROM 86-11 TO 89-6	1989 May 23	41

SUPPLEMENTARY NOTATION

COSATI CODES		
FIELD	GROUP	SUB-GROUP

18 SUBJECT TERMS (Continue on reverse if necessary and identify by block number)
FASINEX
Aircraft Meteorological Measurements
Sea Surface Temperature

ABSTRACT (Continue on reverse if necessary and identify by block number)

Measurements of sea surface temperature during low-level flights by the National Center for Atmospheric Research Electra aircraft and by ships R/V *Endeavor* and R/V *Oceanus*, during the Frontal Air-Sea Interaction Experiment (FASINEX), are combined to map the sea surface temperature field over a 90 by 100 km region on five days of the experiment (16, 17, 18, 21 and 24 February 1986). Distributions of sea surface temperature, interpolated to a regularly spaced grid, are presented in the form of contour maps for each day. The position and intensity of an ocean front, lying within the region, and other features in the sea surface temperature field, are documented. Derivation of sea surface temperature from aircraft measurements, data processing methods, and incorporation of ship measurements are described.

D DISTRIBUTION / AVAILABILITY OF ABSTRACT ☒ UNCLASSIFIED/UNLIMITED ☒ SAME AS RPT ☐ DTIC USERS	21 ABSTRACT SECURITY CLASSIFICATION UNCLASSIFIED
a NAME OF RESPONSIBLE INDIVIDUAL Richard J. Lind	22b TELEPHONE (Include Area Code) (408)646-2674 22c OFFICE SYMBOL 63Ln

D FORM 1473, 84 MAR 83 APR edition may be used until exhausted
All other editions are obsolete

SECURITY CLASSIFICATION OF THIS PAGE
UNCLASSIFIED

ABSTRACT

Measurements of sea surface temperature during low-level flights by the National Center for Atmospheric Research Electra aircraft and by ships R/V Endeavor and R/V Oceanus, during the Frontal Air-Sea Interaction Experiment (FASINEX), are combined to map the sea surface temperature field over a 90 by 100 km region on five days of the experiment (16, 17, 18, 21 and 24 February 1986). Distributions of sea surface temperature, interpolated to a regularly space grid, are presented in the form of contour maps for each day. The position and intensity of an ocean front, lying within the region, and other features in the sea surface temperature field, are documented. Derivation of sea surface temperature from aircraft measurements, data processing methods, and incorporation of ship measurements are described.

TABLE OF CONTENTS

1. INTRODUCTION.

The Frontal Air-Sea Interaction Experiment (FASINEX) was designed to gather information to study the interaction between the ocean and overlying atmosphere. The experiment took place in a region near the Gulf Stream, southwest of Bermuda (centered near 28°N, 70°W), during January, February and March 1986. The region is dominated by a strong ocean surface temperature discontinuity, making the experiment somewhat unique. Stage and Weller (1985, 1986) describe the overall program, its aims, and details of the experiment.

This report focuses on mapping the sea surface temperature (SST) field from measurements made during overflights by an instrumented aircraft, and from ships operating in the flight region. The intent of this work is to identify the position and intensity of the ocean front and the character of the SST field. Ship-based SST measurements were used to supplement aircraft SST data. Combining ship SST measurements with the aircraft data greatly improved the mapping of the sea surface temperature field. Details of how SST's were derived from aircraft measurements, data processing methods, and incorporation of ship data are described.

1.1 NCAR Electra Aircraft Measurements.

The National Center for Atmospheric Research (NCAR) Electra aircraft is equipped with both upward and downward looking Barnes Engineering Co. Precision Infrared Radiometers, models PRT-6 and PRT-5, respectively, among its suite of instruments. The PRT-5 and PRT-6 measure radiance in the wavelength band of 8 to 14 μm (referred to as the "water vapor window"). In this configuration, PRT-5 temperatures are representative of the uppermost ~50 μm of the ocean surface, while temperatures from the PRT-6 are closely related to those of cloud hydrometeors. In the absence of clouds, PRT-6 temperatures tend toward a cold background level (observed to be ~-35°C during FASINEX).

Both sensors operate in a similar manner. Target radiance, observed within a 2° cone, is compared to a temperature-controlled reference cavity radiance by means of a rotating, highly reflective, chopper. The chopper-stabilized difference between target and reference radiance is converted to an analog signal proportional to the target temperature. Signals were digitized and recorded at a rate of one sample per second for the downlooking PRT-5 and 20 samples per second for the uplooking PRT-6 during FASINEX.

The NCAR Electra aircraft completed "box" patterns at an altitude of 30-40 m on five days during FASINEX (16, 17, 18, 21 and 24 February 1986). Severe weather on 20 February, with waterspouts observed, caused the flight on this day to be terminated before completion of the patterns. Flights were composed of 8-10 individual legs running generally north-south (N-S) or east-west (E-W). Patterns covered an area of approximately 90 by 100 km and were intended to be centered over the most recent position of the ocean front. Low-level sampling generally began between 15:00 and 16:00 UT and was completed in 2 to 2-3/4 hours. Figure 1 shows an idealized NCAR Electra flight path for the box patterns and associated legs.

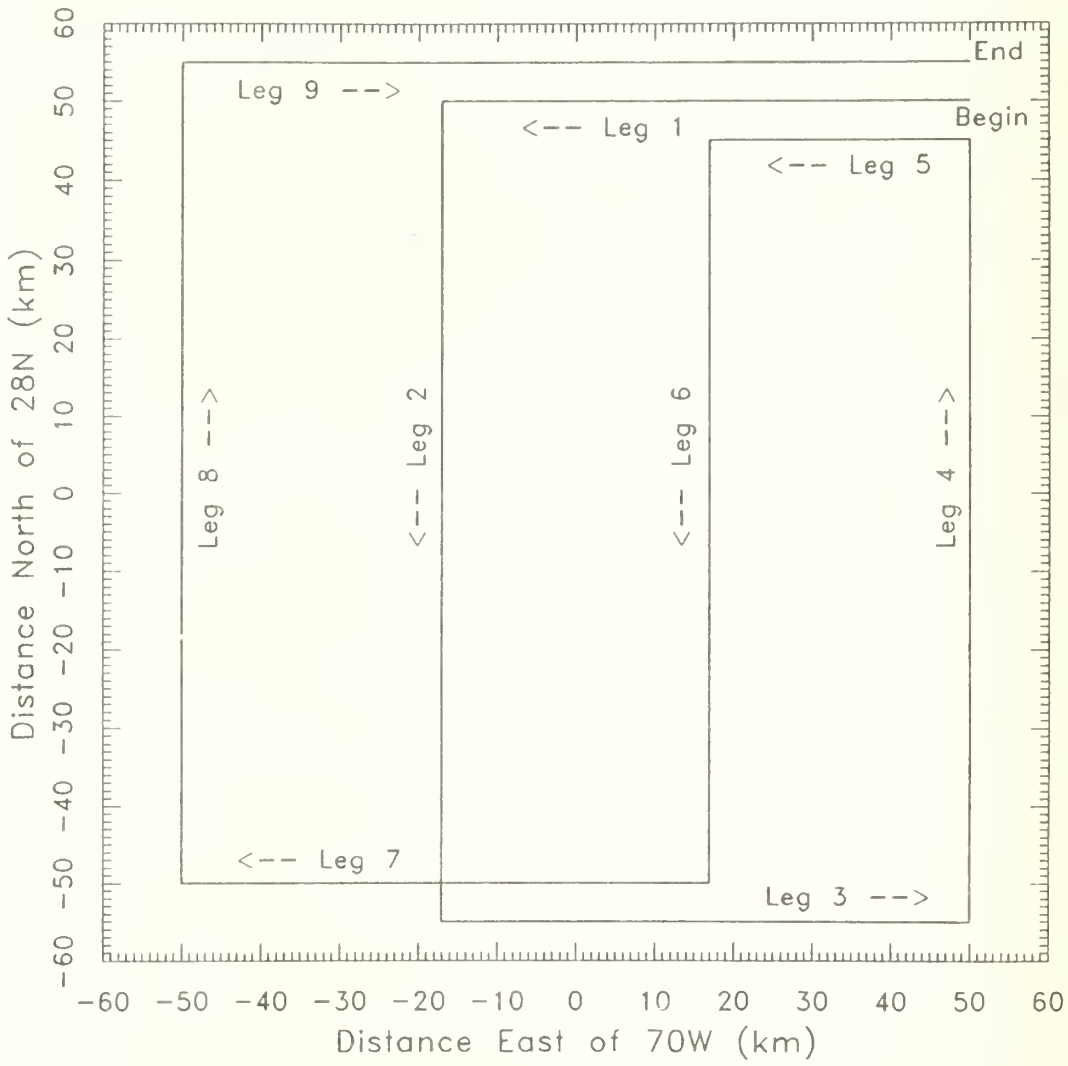

Figure 1. Idealized flight pattern flown by NCAR Electra aircraft during FASINEX. Distances are kilometers from reference position of 28° N, 70° W. Low level sampling generally began with east to west Leg 1 and ended with west to east Leg 9. Overlapping segments of east-west legs (separations are exaggerated for clarity) were used to determine time-dependent drifts in temperature readings from the downlooking PRT-5 infrared thermometer.

Deviations from this idealized flight pattern occurred on 21 and 24 February. To avoid entering reserved air space on the 21st, the last half of Leg 7 was altered. After passing over the intersection of the southern limit of Leg 2, the NCAR Electra turned toward the northwest until intersecting Leg 8. This diagonal leg is referred to as a Leg 7b. On the 24th, the first east to west leg was omitted, and the flight began with a north to south leg in the position of idealized Leg 2. As such, only eight legs were flown on the 24th. The numbering scheme identifies the first leg of this day's flight as Leg 2, and subsequent legs as 3 though 9.

Position information is given as kilometers east and kilometers north of the FASINEX reference position of 28°N, 70°W. In this coordinate system, longitudinal distance is preserved regardless of latitude, making the flight region rectangular. Gradients of measured quantities, expressed in units per km, can be easily calculated from tabulated data and observed from contour plots over the flight region. Appendix A contains algorithms to convert these distances to latitude and longitude, and vice versa.

Position information was derived from the NCAR Electra Inertial Navigation System (INS) with corrections applied to account for errors introduced by the 84.4-min Schuler oscillation and other drifts. The correction method is discussed in Shaw (1988) and details of the correction for NCAR Electra flights during FASINEX are presented in Shaw and Vaucher (1987). The Electra INS positions were used because LORAN-C positions tended to have occasional sharp jumps in both east and north position components.

Corrected INS positions were used to determine start and stop times for individual legs of each box pattern, as well as for overlapping leg segments. These times and the starting and ending positions of each leg are listed in tabular form for each flight day in Appendix B. Data processed were limited to straight-line flight with roll angles less than 4° and at altitudes less than 50 m. These criteria limit potential errors in derived sea surface temperatures due to changes in sensor viewing angle and changes in atmospheric absorption and emittance in the layer between the surface and measurement altitude.

In general, east-west legs partially overlapped on both sides of the ocean front. Separate passes over the same locations allow the determination of time derivatives in the flight data. These comparison passes were used to correct measurements of sea surface temperature for drifts in sensor readings.

1.2 Ship-based Sea Surface Temperature Measurements.

R/V Oceanus (Woods Hole Oceanographic Institution) and R/V Endeavor (University of Rhode Island) operated in the vicinity of the ocean front during the time the NCAR Electra aircraft was completing its flight patterns. Measurements of sea surface temperature were made from both ships and have been tabulated and described by Pennington and Weller (1986).

Sea surface temperatures were measured with three separate sensors on R/V Oceanus and continuously logged at 15-min intervals. These measurements included: manual dipped "bucket" temperatures; a towed, floating temperature sensor from an XBT; and a sensor monitoring engine coolant water intake temperature. Measurements of SST from R/V Endeavor were made by a towed, floating thermistor and were logged continuously at 10-min intervals.

Ship-based water temperature measurements may require correction to represent the topmost "skin" temperature measured by the PRT-5 on the aircraft. Differences between the water temperature just beneath the surface and the skin temperature can range from +0.2 to -0.7°C, depending on conditions near the air-sea interface (Katsaros, 1973). Shipboard SST measurements were made at varying depths: generally 10-50 cm for "bucket" samples; 0-10 cm for towed, surface-skimming sensors; up to 3 m for engine intake water temperature measurements. Errors in ship-based SST measurements can occur due to the presence of the ship. Water samples may be contaminated by warmer, exhausted engine cooling water, or by cooler waters introduced at the surface by upwelling and mixing due to movement of the ship.

The combination of the above-mentioned factors can lead to differences of more than 1°C between ship and aircraft sea surface temperature measurements. Relative changes in temperatures measured by the ships during transits through the flight region should, however, match changes in temperatures observed by the aircraft over the same region. To utilize these ship data in the evaluation of the sea surface temperature field, constant offsets were applied to ship-based SST measurements over each day to force them to match mean aircraft-derived SST measurements.

1.3 Moored Buoy Sea Surface Temperature Measurements.

Moored buoys, with thermistor chains at fixed depths, were installed several months before the NCAR Electra aircraft flew its missions. Positions were based upon the current location of the ocean front and its projected movement. By the time of the aircraft flights in February, the ocean front had moved north of these buoys and outside the boundaries flown by the aircraft. Consequently, measurements from moored buoys could not be combined with aircraft measurements in the determination of the SST field.

2. AIRCRAFT DETERMINATION OF SEA SURFACE TEMPERATURE.

The conversion of raw PRT-5 samples to sea surface temperature requires two distinct steps: 1) correction for non-unity emittance and non-zero reflectance of the sea surface in the measurement wavelength band (sky effects), and 2) correction for sensor temperature drifts.

2.1 Radiation Correction of PRT-5 Temperatures.

Temperatures from the downlooking PRT-5 T_5 are representative of the uppermost ~50 μm of the ocean. The ocean is not radiatively "black" over the water vapor window wavelength band. A portion of the radiance measured by the PRT-5 is composed of reflected radiance from the skyward hemisphere. To convert T_5 to true surface temperature, a correction must be applied. Uplooking PRT-6 temperatures T_6 were used to represent sky radiance, because this sensor measures over the same wavelength band as the downlooking PRT-5.

Sea surface temperature T_{sfc} was calculated from measurements of T_5 and T_6, using (1) with emittance ϵ of 0.986 and reflectance α ($=1-\epsilon$) of 0.014. The value of ϵ is taken from Mikhaylov and Zolotarev (1970).

$$T_{sfc} = \left(\frac{1}{\epsilon} T_5^4 - \frac{\alpha}{\epsilon} T_6^4 \right)^{1/4} \qquad (1)$$

The resulting correction of T_5 to T_{sfc}, from (1), is shown in Figure 2 as a function of T_6, for T_5 = 20°C. The correction is proportional to the difference between sky and surface temperatures. During FASINEX, T_6 ranged from -35 to +10°C, and resulting radiation corrections ranged from +0.6 to +0.1°C.

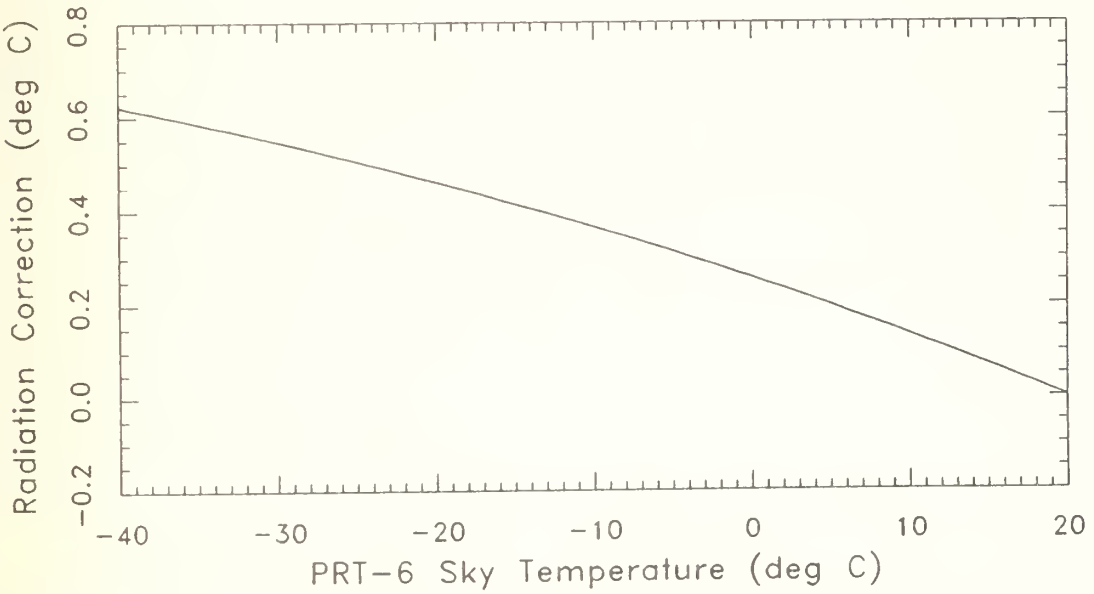

Figure 2. Radiation correction, using (1), applied to downlooking PRT-5 readings to remove influences of sky temperature, sensed by uplooking PRT-6. Curve represents correction for constant PRT-5 temperature of 20° C.

2.1.1 Applying Emittance Correction to Aircraft Data.

The use of (1) with simultaneously sampled data from both upward and downward looking PRT sensors, while removing the gross effects of changing sky conditions from sea surface temperatures, can introduce spurious short-term under- and over-corrections to the computed time series of T_{sfc}. This is most apparent when the aircraft passes beneath the edge of a low cloud and is likely due to the limited solid angle viewed by the uplooking PRT-6. Due to waves on the ocean surface, reflection of sky radiance into the PRT-5 may originate from a portion of the sky not represented by coincident PRT-6 temperature measurements.

Figure 3 shows T_δ and T_θ measurements and T_{sfc} calculated using (1) from Leg 4 of the NCAR Electra flight on 16 February 1986. Cloudiness during this day was characterized by small-scale cumulus having dimensions of a few kilometers. Changes in T_θ of 30°C in less than three seconds were observed at the cloud edges. The over- and undercorrections in T_{sfc} are clearly correlated with the series of T_θ.

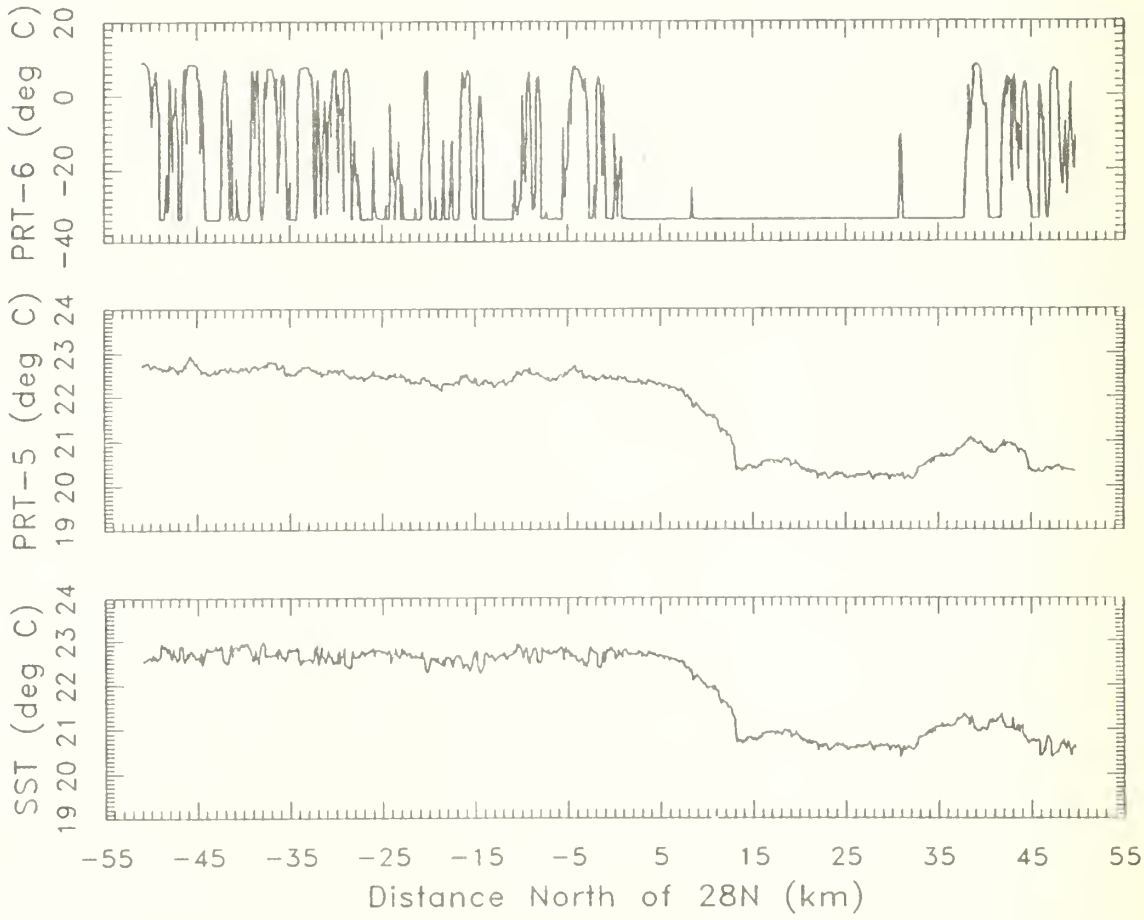

Figure 3. NCAR Electra aircraft one sample per second observations of T_θ from uplooking PRT-6 [top], T_δ from downlooking PRT-5 [middle], and resulting T_{sfc} using (1) [bottom] for south to north Leg 4 on 16 February 1986.

2.1.2 Effect of Filtering PRT-6 Data on Correction.

If data from the uplooking PRT-6 are passed through a 21-second running mean filter, representing approximately 1 km ahead to 1 km behind the aircraft, the data appear to be more representative of the effective sky temperature. Variability in the corrected sea surface temperatures introduced using (1) is greatly reduced. Figure 4 demonstrates the effect of this filtering on T_6 and the effect of its use in (1) on the radiatively corrected T_{sfc}.

Although it is an improvement, this method does not account for sky radiance from left or right of the flight path which may be reflected from the surface into the PRT-5. A hemispheric sensor would be more appropriate to represent the sky temperature field, and an Eppley Precision Infrared Radiometer (model PIR) on the NCAR Electra aircraft could have been used. However, it measures irradiance over a much broader wavelength band (4 to 50 μm) and would introduce undesirable effects, since this wavelength band is much more sensitive to water vapor than the bandwidth of the PRT-6.

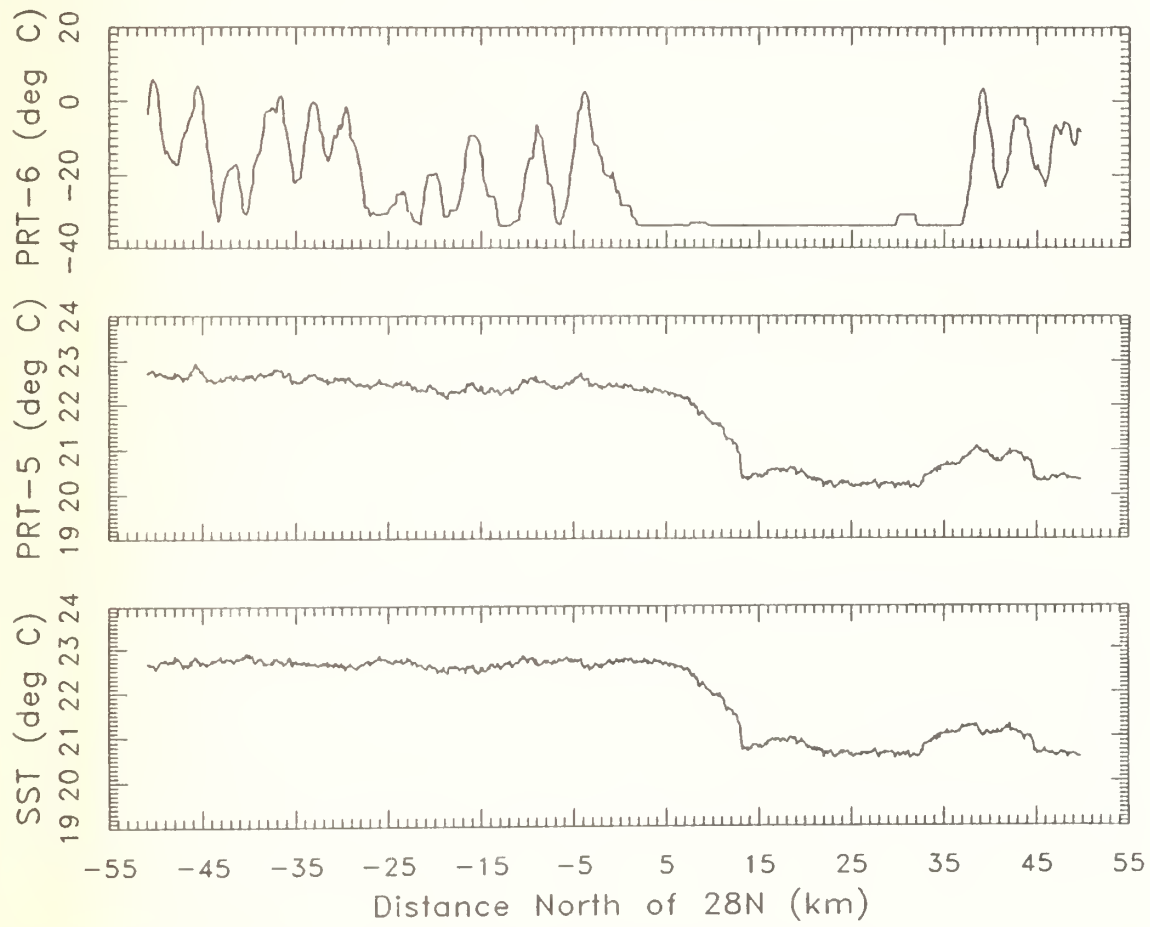

Figure 4. Same as Figure 3, except T_6 has been filtered by a 2-km equal-weighted running mean filter [top] before using (1) to calculate T_{sfc} [bottom].

2.2 Correction for Drift of PRT-5 Signals.

Temperatures derived from the downlooking PRT-5 are generally reliable providing the reference cavity temperature remains stable and at its specified temperature. When comparing measurements from overlapping portions east-west legs, T_{sfc} was observed to slowly drift with time t. T_{sfc} was as much as 1.2°C cooler on later passes over the same water. This drift was also observed to end after one to two hours of low-level sampling.

It is unlikely that there were significant changes (>0.2°C) of T_{sfc} in the time between overlapping leg segments. It is more likely that the reference cavity of the PRT-5 was unable to maintain its temperature during descent from aircraft ferry altitude (with air temperatures ~-20°C) to measurement altitude, (where temperatures were ~+20°C). After sufficient time in this new environment, the cavity temperature appeared to recover to a stable reference value. This would account for the large differences noted early in the flight pattern and explains the stabilization of the readings after a given time in the low-level pattern.

This sudden change of ~40°C undoubtedly affected the PRT-6 measurements, as well. However, an error of 1°C in T_6 contributes less than 0.02°C error to T_{sfc} using (1). Drift corrections were, therefore, only applied to the measurements from the downlooking PRT-5.

For each overlapping leg segment, 30-35 km in length, means were computed for T_{sfc}. These means, and their associated times were used to construct a linear, time-dependent correction scheme to remove drifts in T_{sfc} caused by the PRT-5. This correction, in the form of (2), was only applied between the start of low-level sampling and the time t_{ref} (seconds past 00:00 UT) when T_{sfc} was determined to stabilize.

$$T_{sfc} = T_{sfc} + a\ t + b, \qquad \text{for } t \leq t_{ref} \qquad (2)$$

and,

$$T_{sfc} = T_{sfc}\ , \qquad \text{for } t > t_{ref}$$

Data used to determine T_{sfc} drifts were from overlapping portions of Leg 1, Leg 5 and Leg 9, allowing data to be compared from three separate passes at three distinctly different times. Data from overlapping portions of the first half of Leg 3 and the first half of Leg 7 were also used.

On 24 February 1986, the first leg was not flown and additional data from low-level overlapping flight data, following the completion of the box patterns, were incorporated to compute T_{sfc} drift corrections. Figure 5 shows PRT-5 drifts introduced into T_{sfc} and the fits to these data using (2) for each flight day of FASINEX. Table 1 lists reference times t_{ref} and coefficients a and b, in (2), for each flight day of FASINEX.

Table 1. Coefficients and reference times (seconds past 00:00 UT) of linear time-dependent (2) to correct for drift in T_{sfc} due to drifts in the NCAR Electra downlooking PRT-5 infrared thermometer. Correction is zero for times greater than the reference time t_{ref}.

Date	t_{ref}	a	b
2/16	62632	-2.121E-4	13.29
2/17	60669	-1.577E-4	9.57
2/18	61150	-1.946E-4	11.90
2/21	61471	-1.465E-4	9.01
2/24	62106	-2.217E-4	14.10

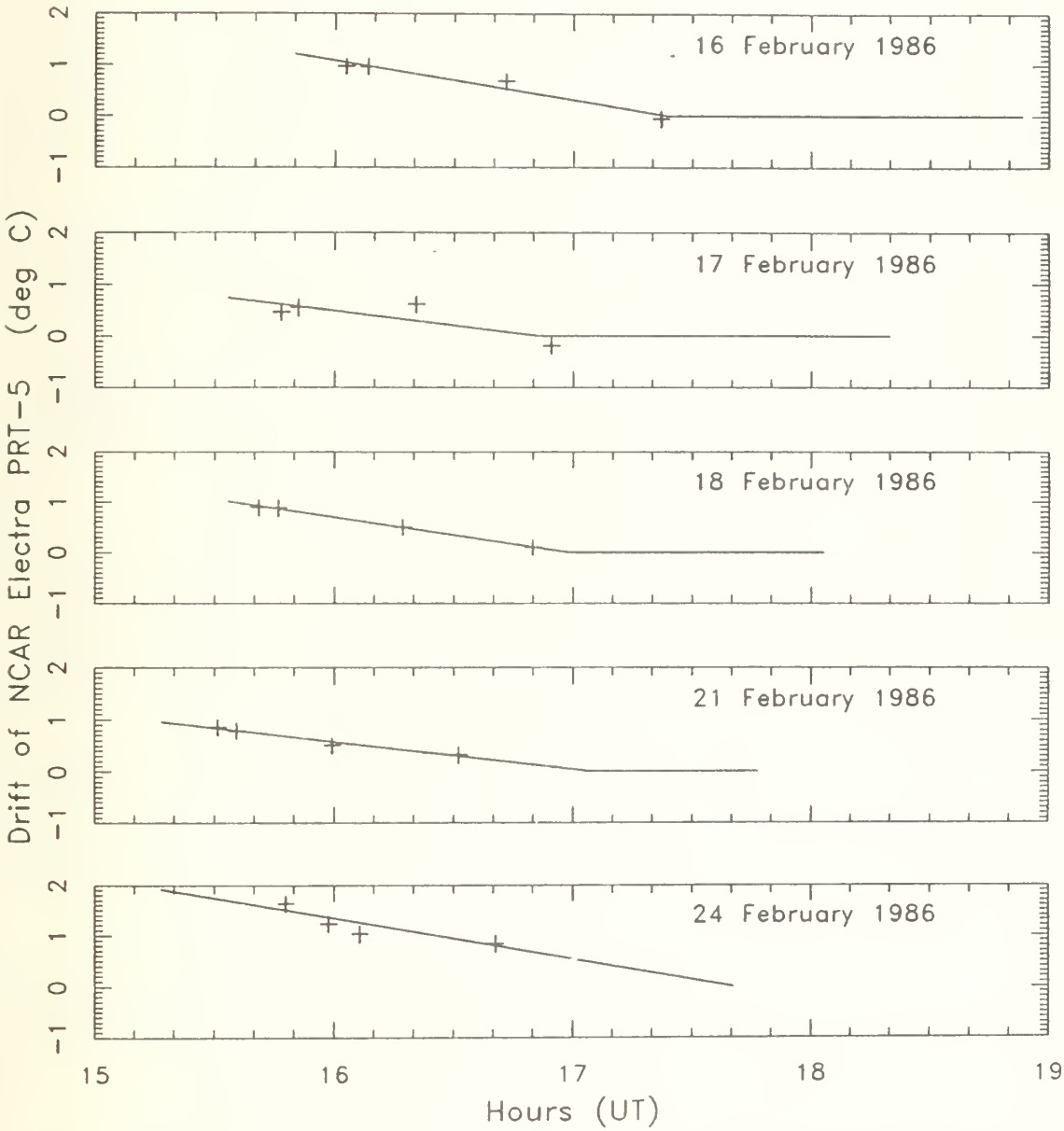

Figure 5. Calculated time-dependent drifts of downlooking PRT-5 temperatures (+) and fit to data (--) for each flight day of FASINEX. Drifts were determined from measurements during overlapping segments of east-west legs of the flight pattern.

3. INCORPORATION OF SHIP SEA SURFACE TEMPERATURE DATA.

This work focuses on documenting the relative changes in sea surface temperature over the flight region for each flight day. Coverage provided by the NCAR Electra aircraft box patterns is limited; north-south legs were separated by 30-35 km and east-west legs were over 100 km apart. Ship-based SST measurements were utilized to supplement coverage provided by the NCAR Electra aircraft. Additional information about the character of the SST field between flight legs is provided by R/V Oceanus and R/V Endeavor SST measurements. Ship-based data were used only when the ship was sampling within the region emcompassed by the flight patterns and were limited to measurements made within a time window of ±6 hours from the mid-flight time of the Electra. To incorporate R/V Oceanus and R/V Endeavor sea surface temperature measurements and aircraft data into a unified data set, constant temperature offsets were applied to the ship measurements to match aircraft observations on each day.

R/V Oceanus made extended transits through the flight region on 16, 17, 18 and 21 February 1986. On the 24th, R/V Oceanus operated in a limited area within a region of large SST gradients. R/V Endeavor measurements tended to be clustered near the ocean front. On 16th and 17th, R/V Endeavor was outside the flight region during the time window, so their SST measurements were not used. Measurements from R/V Endeavor on 18, 21 and 24 February were used in the analysis. Appendix C shows ship positions, along with NCAR Electra flight paths, for each flight day.

3.1 Matching Ship and Aircraft SST Measurements.

Direct ship-aircraft comparisons were made after the aircraft completed its box patterns on two separate days. Comparisons consisted of upwind and downwind flights of ~30 km length centered over ship positions. On both days, each ship was operating in the vicinity of significant SST gradients, greater than 0.5°C/km in one comparison leg, making these comparison data difficult to interpret.

The NCAR Electra also flew over positions sampled by one or both ships on all flight days. Although there may be time differences of up to seven hours between ship and aircraft SST measurements at each location, these comparison data were used to match ship and aircraft measurements. Table 2 lists adjustments applied to ship SST measurements for each flight day.

Table 2. Temperature adjustments (° C) added to R/V Endeavor and R/V Oceanus measurements of sea surface temperature to match aircraft-determined measurements for each flight day in FASINEX.

Date	R/V Endeavor	R/V Oceanus
2/16	not used	-0.75
2/17	not used	-1.15
2/18	-1.15	-1.35
2/21	-0.15	-0.45
2/24	-1.10	-0.95

4. REPRESENTATION OF SEA SURFACE TEMPERATURE FIELD.

It is desirable to present areal distributions of sea surface temperature in the form of a regularly spaced grid. This form is convenient for use in model applications, and contouring routines require input data to be spaced at regular intervals.

4.1 Sea Surface Temperature Grid.

The area encompassed by the NCAR Electra aircraft flight pattern on each flight day defined the grid region. The grid comprises 10 east-west columns and 44 north-south rows. Spacing between grid columns is approximately 10 km, and grid rows are separated by roughly 2.5 km. North-south resolution was chosen to be greater because the ocean front was generally aligned in an east-west direction. Resolution between east-west grid points was limited to 10 km because of the lack of information between north-south flight legs. Any further increase in east-west resolution would not necessarily improve the accuracy of the interpolated SST field. The locations of these grid points for each day are shown in Appendix C along with NCAR Electra flight paths and ship positions used in the analyses.

4.2 Interpolation of SST to Grid Positions.

The sea surface temperature at each grid point was calculated by examining corrected aircraft and adjusted ship-based SST measurements within a specified region of influence surrounding each grid point location. A spline surface of SST was fit to this region of influence using an over-relaxation process, and the value at the grid point was evaluated. A subroutine from the PLOT88 software library (Plotworks, Inc., La Jolla, CA) was used in the interpolation algorithm.

The dimensions of this rectangular region of influence were changed according to the density of measurements. In areas of the flight region where only aircraft data were available, the influence region was set to be ~8 km N (high) by ~30 km E (wide). The relatively large width insured that data from at least two north-south legs were included in the region of influence for grid points between flight legs. One of the drawbacks of using such an elongated region is that SST features in the north-south flight legs tend to be stretched in the east-west direction.

Where ship data were available for use within a portion of the aircraft flight region, the region of influence for these grid points was set to be ~12 km N by either ~18 or ~25 km E, depending on the density of measurements. This adjustment to the region of influence helped to reduce the artificial east-west elongation of features in the SST field.

Input data to the grid interpolation algorithm consisted of a mix of unaveraged (1-sec) and 5-km averaged aircraft SST data, and adjusted ship-based SST measurements within the flight area (limited to ±6 hrs of the aircraft mid-point time). Averaging the data reduced the number of

points involved in the determination of each spline surface. The inclusion of unaveraged aircraft data was limited to areas where SST gradients were large. These additional high resolution SST data greatly enhanced the reproduction of details within the ocean front by the grid data.

Sea surface temperature grid data are presented in tabular form in Appendix D for each flight day. These data are also available from the authors on magnetic media. It is hoped that these regularly spaced SST grid data will provide a reference database which will be useful to FASINEX investigators.

4.3 Contouring of Sea Surface Temperature Grid Data.

Contours of constant sea surface temperature were drawn by interpolating between grid point locations over the flight region. Areas having dimensions of 2.5 km N by 10 km E, centered over each grid point, were divided into 16 sub-grid areas and spline surfaces were fit to each sub-grid area. Straight line segments were drawn between the intersections of each sub-grid surface and the chosen contour intervals.

Intervals of 0.3°C were used in the contouring. With this interval, gradients in the SST field are easily identified without losing individual contours in a "sea of black ink" along the ocean front. Contour plots of sea surface temperatures for each flight day are shown in Appendix E.

In our application of the contouring subroutine (from the PLOT88 software library), no smoothing was applied to the grid data. The "wall" in SST at the ocean front, seen in unaveraged aircraft data for most north-south flight legs, would appear more "ramp-like" if smoothing had been applied. Some of the smaller details in areas devoid of measurements, are probably due to not smoothing the data before contouring.

5. COMPARISON OF GRID DATA WITH AIRCRAFT AND SHIP DATA.

To determine if features of the SST field are accurately reproduced by the sea surface temperature grid data, comparisons between grid data and measurements of T_{sfc} were made. Although it is expected that grid data should compare favorably with the data used to create it, the ability of the grid data to accurately reproduce features in the SST field is a valid test of the methods used.

5.1 Aircraft and Grid Sea Surface Temperatures.

The gross character of the SST field should be accurately represented by the SST grid data. Details of SST patterns, seen in individual aircraft flight legs, are well reproduced by these grid data. Figure 6 shows unaveraged (1-sec) aircraft observations of T_{sfc} from Leg 6 and the nearest corresponding column of SST grid data for each flight day of FASINEX. Gradients in the region of the ocean front are accurately depicted by the SST grid data, and small-scale features are well reproduced.

5.2 Ship and Grid Sea Surface Temperatures.

Sea surface temperature grid data reproduce aircraft SST measurements quite well, but these comparisons only offer validity over the positions of the flight legs. To determine if grid data accurately represent the SST field in the regions between flight legs, comparisons were made between ship-based SST measurements and the SST grid data. Figure 7 shows R/V Oceanus SST measurements and SST's from the nearest corresponding grid column for all flight days. R/V Endeavor data are also shown for 21 and 24 February. Although there are significant temperature offsets, adjusted before use in the grid interpolation algorithm, the position and intensity of the front are well reproduced by the SST grid data.

5.2.1. Potential Errors Introduced Using Ship Data.

Measurements from the ships were used when they were made within a 12 hour period centered on the mid-time of the Electra flight patterns. This was a compromise between obtaining a "snap-shot" of the SST field, with limited aircraft coverage, and using as much ship data as possible. Changes in the SST field over 12 hours may be significant, as currents in the region may move features in the SST field many kilometers over this time period. The differences in the SST field between the 17th and 18th of February (Appendix E) is a good example of changes that can occur in just 24 hours.

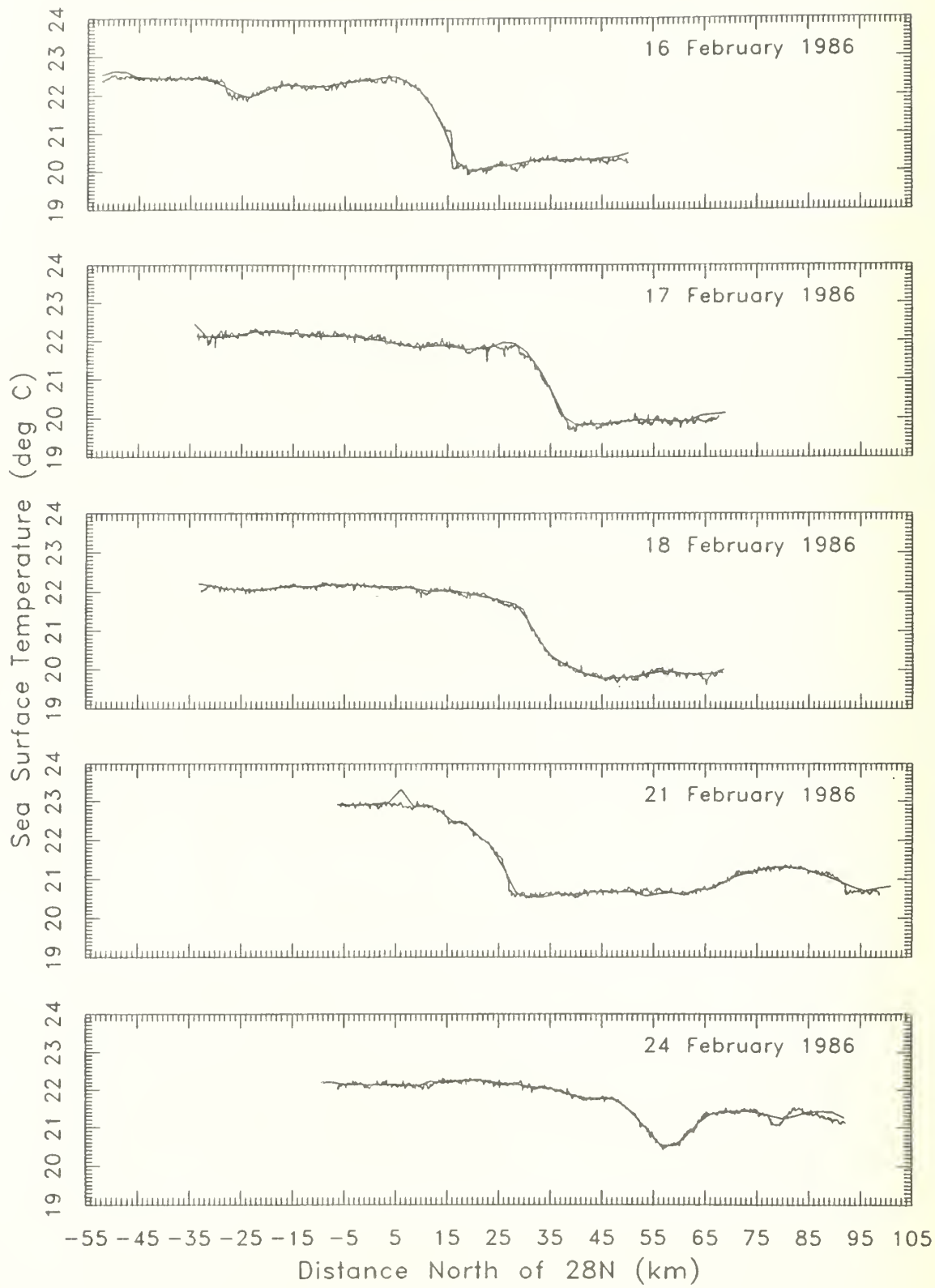

Figure 6. One sample per second sea surface temperature measurements from north to south Leg 6 of NCAR Electra flights and column of SST grid data closest leg position for each flight day of FASINEX. Leg 6 was located ~15 km east of 70° W on all flight days.

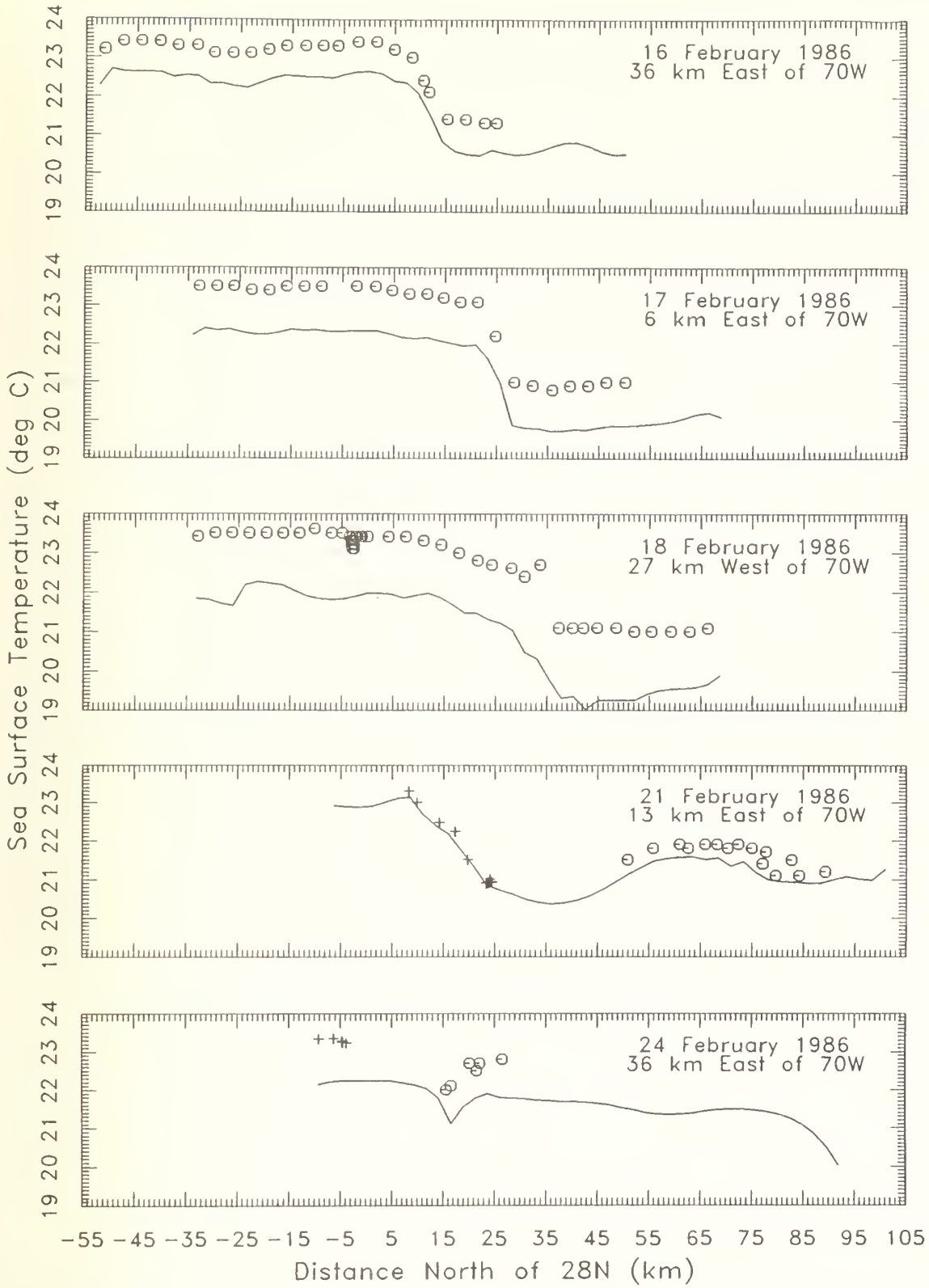

Figure 7. Sea surface temperature measurements from R/V Endeavor (+) and R/V Oceanus (o), and column of SST grid data (--) closest to ship locations for each flight day of FASINEX. Constant offsets, listed in Table 2, were applied to ship data before inclusion in data set. Distances east of 70° W for each north-south grid column are listed in the upper right-hand portion of each frame.

There was only one series of ship measurements made along an aircraft flight leg. On 18 February, R/V Endeavor measurements were concentrated over the ocean front on the western edge of the flight area. Figure 8 shows Leg 8 aircraft data, R/V Endeavor measurements, and the SSTs from the closest corresponding column of grid data. These measurements were all within ±1 km (east-west) of each other (measurement locations are shown in Appendix C). Electra measurements were from 17:36 to 17:44 UT for this segment, while R/V Endeavor measurements were made between 10:50 and 12:10 at 42-44 km north of 28°N, 13:30 and 16:40 at 51-54 km, and 22:00 and 23:00 at 60-62 km.

There appears to be a distance offset of 5-8 km between ship and aircraft SST measurements. However, there are indications that warmer water was advecting into this region from the west, and that the ocean front was moving north during this period. R/V Endeavor measurements between 22:00 and 23:00 (60-62 km) could, therefore, be representative of water on the warm side of the ocean front.

The corresponding column of SST grid data, shown in Figure 8, shows the effect of including these R/V Endeavor measurements in the grid interpolation algorithm. There is a 0.3-0.4°C difference between Electra data and grid data at 52 km, and grid data are 0.1-0.2°C higher than Electra data at 61 km. These differences indicate the magnitude of errors that may be introduced by incorporating ship SST measurements into the data set.

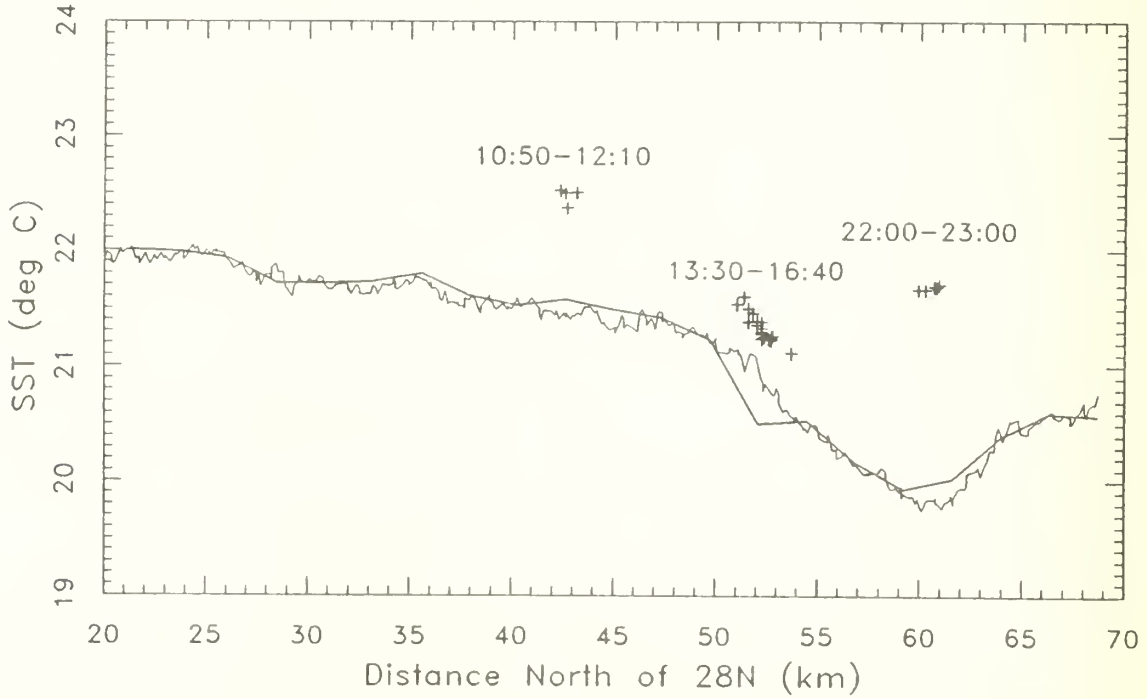

Figure 8. One sample per second sea surface temperature measurements from portion south to north Leg 8 of NCAR Electra flight of 18 February, column of SST grid data closest to leg position (--), and R/V Endeavor SST measurements (+) within ± 1 km of of flight track. R/V Endeavor measurement times are listed above each cluster of points. Aircraft measurements were made between 17:36 and 17:44 UT.

6. DISCUSSION.

The data presented in this report show the variability of the sea surface temperature field over the area encompassed by the NCAR Electra flight patterns. We believe that the relative spatial changes of SST are accurate. However, there were insufficient intercomparison data available to establish the absolute accuracy of the daily mean SST. Therefore, ship data have been incorporated by adding an appropriate temperature offset such that the mean value of ship-derived SST's agree with the mean value of aircraft SST's for collocated ship and aircraft positions. Users of these data may wish to adjust the mean sea surface temperatures for a given day for comparison with other observations.

6.1 Discussion of Errors.

Errors in the SST field can arise due to (1) errors in temperatures input to the grid interpolation algorithm, (2) errors in platform positions, (3) movement of surface waters by currents within the time window of observations, and (4) application of the interpolation and contouring methods.

6.1.1 Temperature Errors.

Potential sources of errors in T_{sfc}, used as input to the interpolation algorithm, include (1) contamination of aircraft PRT-5 temperatures due to the reflection of 8 to 14 μm radiance from the skyward hemisphere, (2) drifts in aircraft PRT-5 temperatures, and (3) incorporation of ship SST measurements, made just below the surface, with the aircraft-derived skin temperature measurements.

In Section 2.1, corrections for reflection of sky radiance were made ranging from +0.6 to +0.1°C. After passing uplooking PRT-6 data through a 21-second equal-weighted running mean filter, corrected T_{sfc} values show little correlation with the sky temperature. It is estimated that residual errors from this source are of the order of 0.1°C.

Errors due to PRT-5 temperature drifts in the PRT-5 were addressed in Section 2.2. Relative errors over the flight region were reduced substantially by the drift correction, making aircraft-derived T_{sfc} self-consistent over the flight region. Exponential fits to the comparison data would have been more appropriate if the time scales of the drifts were shorter. The linear correction scheme removes a large portion of the error, and residual errors, based on comparisons between the correction and the measured drifts, are ~0.2°C.

The constant temperature offsets applied to the ship-based SST measurements to match aircraft-derived measurements of the skin temperature, listed in Table 2, were not consistent from day to day. Differences between the skin temperature and those at the depths of ship SST measurements could be as large as 0.7°C, and it is expected that these differences can change across the flight region, due to changing conditions, as well as from day to day. Matching the ship-based and

aircraft T_{sfc} measurements was only done to allow data from all platforms to be utilized. Errors introduced by the inclusion of ship data are estimated to be less than 0.5°C, as discussed in Section 5.2.1.

6.1.2 Position Errors.

Errors in the positioning of the ocean front and other features in the SST field may arise from (1) errors in the NCAR Electra inertial navigation system, (2) errors in ship position data, and (3) movement of the surface waters, by currents, throughout the sampling period for each day.

After correction for the 84.4-min Schuler oscillation, by Shaw and Vaucher (1987), NCAR Electra INS positions are considered to be as accurate as the LORAN-C positions. Specified accuracy for the LORAN-C position, over the FASINEX region, is about 500 m for each sample (U. S. Coast Guard, 1980). Using 10-sec averaged LORAN-C positions to correct aircraft INS positions reduces this error to ~100 m. Both ships logged their positions using LORAN-C at 10 or 15-min intervals, so positions should be accurate to 500 m.

Surface currents in the FASINEX area may introduce errors in the positioning of features in the SST field due to the extended period of measurements (±6 hours from the mid-point time of aircraft sampling). If currents are steady at ~10 cm s^{-1}, surface waters can move ~5 km between measurements at the start and end of this period. Ship-based SST measurements could be representative of temperatures several kilometers distant from those measured by the aircraft. For aircraft sampling, over a period of less than three hours, movement of the surface water, by currents, is much less. Section 5.2.1 discussed the effects of positioning errors on the interpolated SST field.

6.1.3 Interpolation Errors.

Although the agreement between SST grid and aircraft data is good, as seen in Figure 6, the interpolation scheme may introduce errors in areas devoid of data due to the constraints of the algorithm. In general, the scheme tends to weaken temperature gradients in these areas, as the region of influence was generally larger than the dimensions of the ocean front. The position of the ocean front in these areas may be in error by as much as 10 km when there is significant curvature in the front.

One example of a potential interpolation error may be seen in the SST contour plot for 17 February (Figure E2). Aircraft data from north-south Leg 6 (flown ~15 km E of 70°W) showed the front ~35 km N of 28°N, while Leg 4 (~45 km E of 70°W) placed the front ~18 km N of 28°N. Measurements from R/V Oceanus, during a north-south transit ~6 km E of 70°W, showed the front ~25 km N of 28°N. The gridding algorithm was forced to fit a series of spline surfaces over this region where the front curves significantly. Although the SST grid data agree with all the measurements, a free-hand analysis of the front in this region would keep the gradient of the front constant, and tend to tighten the

curvature. The actual position of the front between Leg 4 and Leg 6 may be quite different that depicted in Figure E2.

The cold pool of water centered at ~15 km E and ~58 km N of 28°N, 70°W on 24 February (Figure E5) is another example of the "imagination" of the interpolation algorithm. Only data from Leg 6 (seen in Figure 6) showed any evidence of this cold pool. The shape of this feature, with eastward dimensions larger than northward dimensions, is primarily due to the shape of the region of influence used in the interpolation algorithm. If the region of influence had been square-shaped, the cold pool would appear more circular in shape. Without other supporting information, however, the true dimensions of this cold pool are unknown.

The SST field on the 24th may have contained other warm or cold eddies that were not observed along the aircraft flight paths or by the ships. Combining these results with satellite-based observations, such as those presented by Bohm and Cornillon (1987), can help to resolve some of these uncertainties.

6.2 Conclusion.

Changes between 16 and 24 February indicate that there was a significant evolution of the SST field. Whether these changes are due to water moving through the region over the course of the experiment, or due to forcing mechanisms, or a combination of both, cannot be addressed within the scope of this work. Halliwell et al. (1987) have presented maps of the ocean front, derived from satellite imagery and ship and aircraft measurements, for all the days of FASINEX. Their work documents the movement and evolution of the ocean front within a region much larger than the coverage provided by the aircraft. It is hoped that the documentation of the structure of the SST field, presented here, will provide useful information to FASINEX investigators working to understand sea-air processes in this region.

7. REFERENCES.

Bohm, E. and P. Cornillon, 1987: An atlas of AVHRR/2 images from the FASINEX experiment. Tech. Rept. No. 87-3, Graduate School of Oceanography, Univ. of Rhode Island, 77pp.

Halliwell, V. M., E. Bohm and P. Cornillon, 1987: Ship-, satellite- and air-derived sea surface temperature fronts for FASINEX. Tech. Rept. No. 87-4, Graduate School of Oceanography, Univ. of Rhode Island, 115 pp.

Katsaros, K. B., 1973: Supercooling at the surface of an arctic lead. J. Phys. Ocean., 3, 482-486.

Mikhaylov, B. A. and V. M. Zolotarev, 1970: Emissivity of liquid water, Atmos. and Ocean Phys., 6, 52.

Pennington, N. J. and R. A. Weller, 1986: FASINEX Frontal Air-Sea Interaction Experiment (January-June 1986); Cruise Summaries for FASINEX Phase Two: R/V Oceanus Cruise 175, R/V Endeavor Cruise 141, Woods Hole Oceanog. Inst. Tech. Rept. WHOI-86-36, 174 pp.

Shaw, W. J., 1988: Inertial drift correction for aircraft-derived wind fields. J. Atmos. Ocean. Tech., 5, 774-782.

_____ and G. T. Vaucher, 1987: Correction of the wind field measured by the NCAR Electra during FASINEX for inertial navigation system drifts. Tech. Rept. NPS-63-87-008, Naval Postgraduate School, Monterey, CA. 43 pp.

Stage, S. A. and R. A. Weller, 1985: The Frontal Air-Sea Interaction Experiment (FASINEX); Part I: Background and scientific objectives. Bull. Am. Meteor. Soc., 66, 1511-1520.

_____ and _____, 1986: The Frontal Air-Sea Interaction Experiment (FASINEX); Part II: Experimental plan. Bull. Am. Meteor. Soc., 67, 16-20.

U. S. Coast Guard, 1980: LORAN-C User Handbook. Department of Transportation, COMDTINST M16562.3 (old CG-462), 63 pp.

APPENDICES: ORGANIZATION.

Appendix A contains algorithms to convert between latitude and longitude and distances north and east, respectively, of FASINEX reference position 28°N, 70°W. Appendix B lists starting and ending times and positions for low-level flight legs flown by the NCAR Electra aircraft during FASINEX. Figures in Appendix C show locations of aircraft flight legs, and R/V Endeavor and R/V Oceanus positions included in the analyses for each flight day in FASINEX. Locations of regularly spaced grid points are also shown. Appendix D lists sea surface temperature grid data for each flight day, as well as positions of each grid point. Appendix E contains plots of the sea surface temperature contours over the aircraft flight region for each day.

A. CONVERSION BETWEEN DISTANCE AND POSITION.

The algorithm LATLON may be used to convert north-south and east-west distances from the FASINEX reference position of 28°N, 70°W (used thoughout this report) to latitude and longitude. Subroutine XYPOS is an algorithm to convert latitude and longitude to distances north and east, respectively, of the FASINEX reference position. Constant R is the earth's radius (in km), and DTOR is a factor used in the conversion between degrees and radians. DLAT and DLON are degrees of latitude and longitude, and XKM and YKM are in km.

```
      SUBROUTINE LATLON(YKM,XKM,DLAT,DLON)
C        CALCULATES LATITUDE, LONGITUDE FROM INPUT
C        OF DY,DX (IN KM) RELATIVE TO 28N, 70W
      DATA R/6371.0/,DTOR/0.0174533/
      DLAT = YKM / (R * DTOR) + 28.0
      DLON = XKM / (R * COS(DLAT*DTOR) * DTOR) - 70.0
      RETURN
      END

      SUBROUTINE XYPOS(DLAT,DLON,YKM,XKM)
C        RECEIVES LATITUDE AND LONGITUDE IN DECIMAL DEGREES
C        RETURNS POSITION EAST AND NORTH OF 28N, 70W IN KM
      DATA R/6371.0/,DTOR/0.0174533/
      YKM = R * DTOR * (DLAT - 28.0)
      XKM = R * COS(DLAT*DTOR) * DTOR * (DLON + 70.0)
      RETURN
      END
```

B. NCAR ELECTRA FLIGHT LEG TIMES AND POSITIONS.

The tables that follow list starting and ending: times, distances north and east of the FASINEX reference position, and latitudes and longitudes of NCAR Electra low-level flight legs flown during FASINEX.

Table B1. Leg start and stop times and positions for NCAR Electra aircraft flight on 16 February 1986. Times are coordinated Universal Time (UT). Distances are km north, and km east of reference position 28° N, 70° W. Flight path is shown in Appendix C.

	Start	Distance		Position		Stop	Distance		Position	
Leg	Time	N(km)	E(km)	Lat(N)	Lon(E)	Time	N(km)	E(km)	Lat(N)	Lon(E)
1	16:01:05	49.041	45.291	28.441	-69.537	16:10:35	48.396	-14.501	28.435	-70.148
2	16:17:03	48.597	-14.647	28.437	-70.150	16:32:48	-51.740	-12.995	27.535	-70.132
3	16:40:32	-51.934	-12.777	27.533	-70.130	16:50:45	-50.524	45.371	27.546	-69.540
4	16:56:02	-50.813	45.841	27.543	-69.535	17:13:42	49.708	45.461	28.447	-69.535
5	17:19:46	49.715	45.833	28.447	-69.531	17:24:28	50.059	15.780	28.450	-69.839
6	17:31:22	50.223	15.281	28.452	-69.844	17:47:57	-51.984	16.026	27.532	-69.837
7	17:54:18	-52.086	16.070	27.532	-69.837	18:03:44	-52.077	-42.704	27.532	-70.433
8	18:10:20	-52.147	-43.033	27.531	-70.436	18:28:01	49.982	-43.456	28.449	-70.444
9	18:33:47	50.316	-43.548	28.452	-70.445	18:49:13	49.035	45.175	28.441	-69.538

Table B2. Leg start and stop times and positions for NCAR Electra aircraft flight of 17 February 1986. Times are coordinated Universal Time (UT). Distances are km north, and km east of reference position 28° N, 70° W. Flight path is shown in Appendix C.

	Start	Distance		Position		Stop	Distance		Position	
Leg	Time	N(km)	E(km)	Lat(N)	Lon(E)	Time	N(km)	E(km)	Lat(N)	Lon(E)
1	15:44:37	68.702	45.879	28.618	-69.530	15:53:07	68.685	-14.102	28.618	-70.144
2	15:57:17	68.946	-14.331	28.620	-70.147	16:13:32	-32.934	-12.640	27.704	-70.128
3	16:18:07	-33.123	-12.402	27.702	-70.126	16:28:07	-33.100	46.940	27.702	-69.523
4	16:32:19	-33.338	47.345	27.700	-69.519	16:48:04	67.682	46.749	28.609	-69.521
5	16:52:09	67.632	46.792	28.608	-69.521	16:57:05	67.656	15.465	28.608	-69.842
6	17:04:46	67.706	15.695	28.609	-69.839	17:22:24	-33.625	15.767	27.698	-69.840
7	17:26:59	-33.271	18.344	27.701	-69.814	17:36:24	-34.137	-41.777	27.693	-70.424
8	17:39:54	-34.210	-43.904	27.692	-70.446	17:56:00	65.724	-42.393	28.591	-70.434
9	17:59:14	65.957	-42.501	28.593	-70.435	18:15:59	66.224	46.583	28.596	-69.523

Table B3. Leg start and stop times and positions for NCAR Electra aircraft flight on 18 February 1986. Times are coordinated Universal Time (UT). Distances are km north, and km east of reference position 28° N, 70° W. Flight path is shown in Appendix C.

	Start	Distance		Position		Stop	Distance		Position	
Leg	Time	N(km)	E(km)	Lat(N)	Lon(E)	Time	N(km)	E(km)	Lat(N)	Lon(E)
1	15:38:58	68.080	42.470	28.612	-69.565	15:48:39	68.737	-17.260	28.618	-70.177
2	15:52:48	69.920	-18.571	28.629	-70.190	16:10:54	-31.184	-15.336	27.720	-70.156
3	16:14:51	-32.217	-16.385	27.710	-70.166	16:24:42	-32.078	42.072	27.712	-69.573
4	16:28:46	-31.877	45.944	27.713	-69.533	16:43:38	67.293	44.643	28.605	-69.543
5	16:47:28	68.346	45.780	28.615	-69.531	16:52:34	67.891	14.446	28.611	-69.852
6	16:55:36	68.503	13.452	28.616	-69.862	17:13:44	-31.687	13.627	27.715	-69.862
7	17:17:00	-33.001	14.544	27.703	-69.852	17:26:27	-32.856	-45.886	27.705	-70.466
8	17:28:51	-34.413	-46.999	27.691	-70.477	17:43:59	67.611	-47.375	28.608	-70.485
9	17:45:50	68.459	-48.695	28.616	-70.499	18:00:35	67.201	40.352	28.604	-69.587

Table B4. Leg start and stop times and positions for NCAR Electra aircraft flight on 21 February 1986. Times are coordinated Universal Time (UT). Distances are km north, and km east of reference position 28° N, 70° W. Flight path is shown in Appendix C.

	Start	Distance		Position		Stop	Distance		Position	
Leg	Time	N(km)	E(km)	Lat(N)	Lon(E)	Time	N(km)	E(km)	Lat(N)	Lon(E)
1	15:28:50	93.815	51.558	28.844	-69.471	15:38:15	94.324	-10.310	28.848	-70.106
2	15:40:19	92.226	-9.944	28.829	-70.102	15:54:43	-4.652	-9.076	27.958	-70.092
3	15:56:41	-5.000	-10.272	27.955	-70.105	16:06:44	-6.075	48.977	27.945	-69.501
4	16:09:13	-6.570	49.678	27.941	-69.494	16:27:11	96.120	51.425	28.864	-69.472
5	16:29:17	96.491	51.820	28.868	-69.468	16:33:32	98.626	24.028	28.887	-69.753
6	16:35:26	98.606	23.303	28.887	-69.761	16:50:46	-5.743	22.221	27.948	-69.774
7	16:52:47	-6.349	21.677	27.943	-69.779	16:57:27	-5.905	-8.988	27.947	-70.091
7b	16:58:11	-4.044	-12.752	27.964	-70.130	17:05:29	32.457	-37.635	28.292	-70.384
8	17:07:34	32.571	-37.531	28.293	-70.383	17:19:01	100.694	-36.502	28.906	-70.375
9	17:20:54	100.012	-38.121	28.899	-70.392	17:36:08	99.230	51.438	28.892	-69.472

Table B5. Leg start and stop times and positions for NCAR Electra aircraft flight on 24 February 1986. Times are coordinated Universal Time (UT). Distances are km north, and km east of reference position 28° N, 70° W. Flight path is shown in Appendix C.

	Start	Distance		Position		Stop	Distance		Position	
Leg	Time	N(km)	E(km)	Lat(N)	Lon(E)	Time	N(km)	E(km)	Lat(N)	Lon(E)
2	15:22:00	90.427	-23.858	28.813	-70.245	15:39:11	-7.825	-14.511	27.930	-70.148
3	15:42:08	-8.169	-18.180	27.927	-70.185	15:52:14	-9.498	44.698	27.915	-69.545
4	15:55:03	-9.738	45.126	27.912	-69.541	16:10:43	92.013	45.129	28.827	-69.537
5	16:13:17	92.026	45.378	28.828	-69.534	16:18:16	91.989	16.020	28.827	-69.836
6	16:21:44	92.274	15.780	28.830	-69.838	16:39:21	-6.103	15.828	27.945	-69.839
7	16:42:10	-6.978	15.139	27.937	-69.846	16:52:54	-6.136	-44.281	27.945	-70.451
8	16:55:06	-6.124	-44.307	27.945	-70.451	17:10:08	90.160	-43.050	28.811	-70.442
9	17:12:33	90.292	-42.890	28.812	-70.440	17:26:15	90.644	45.047	28.815	-69.538

C. AIRCRAFT FLIGHT PATH, SHIP AND GRID LOCATIONS.

The following figures show locations of NCAR Electra flight paths for each day of FASINEX. R/V Endeavor and R/V Oceanus positions for each day are shown, when measurements of sea surface temperature were included in the analyses. Locations of the regularly spaced grid are also shown, for reference.

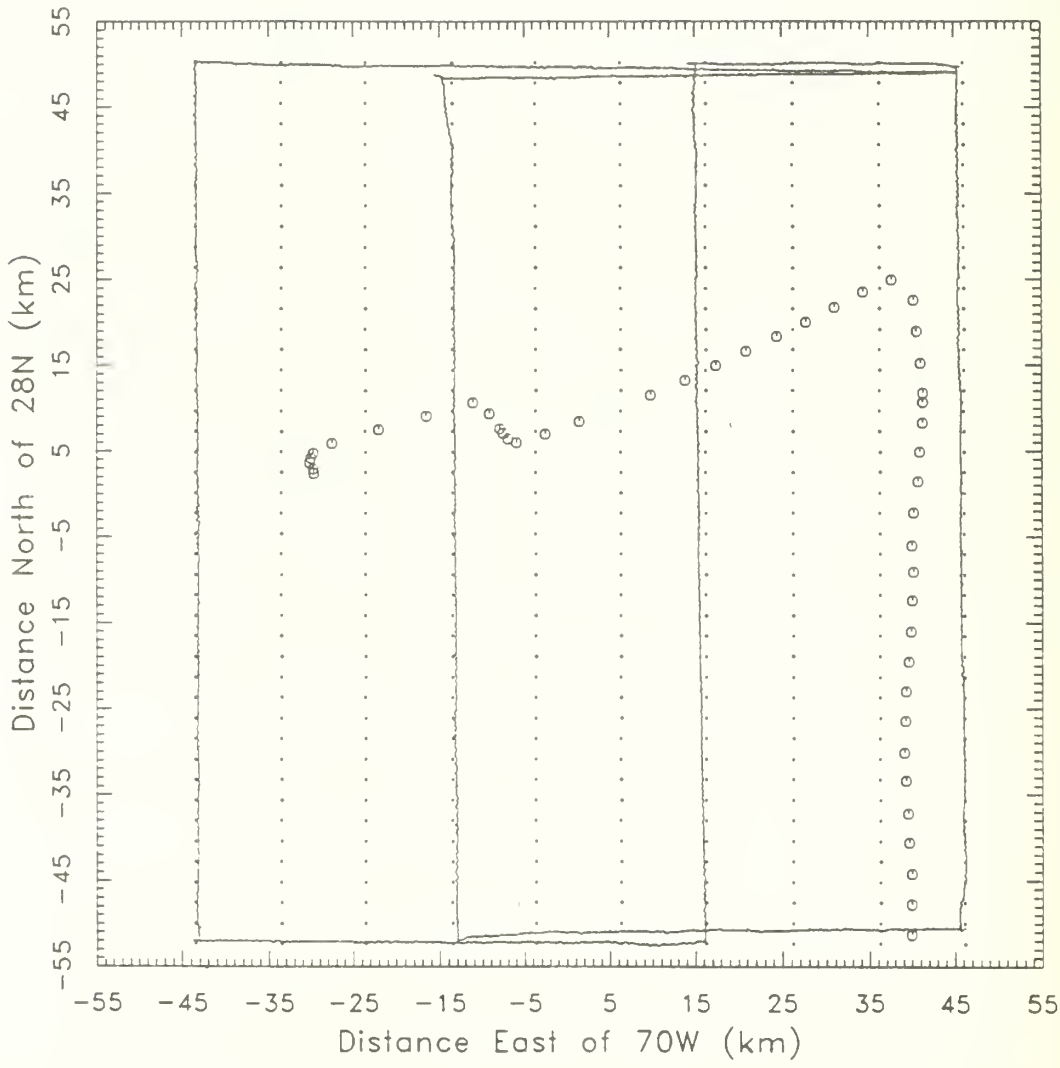

Figure C1. Flight pattern flown by NCAR Electra aircraft (--) on 16 February 1986, positions of R/V Oceanus (o) where sea surface temperature measurements were included in the analysis, and locations of regularly spaced (10 by 44) grid points (•). Distances are kilometers from reference position of 28° N, 70° W. R/V Endeavor was operating outside the flight region on this day.

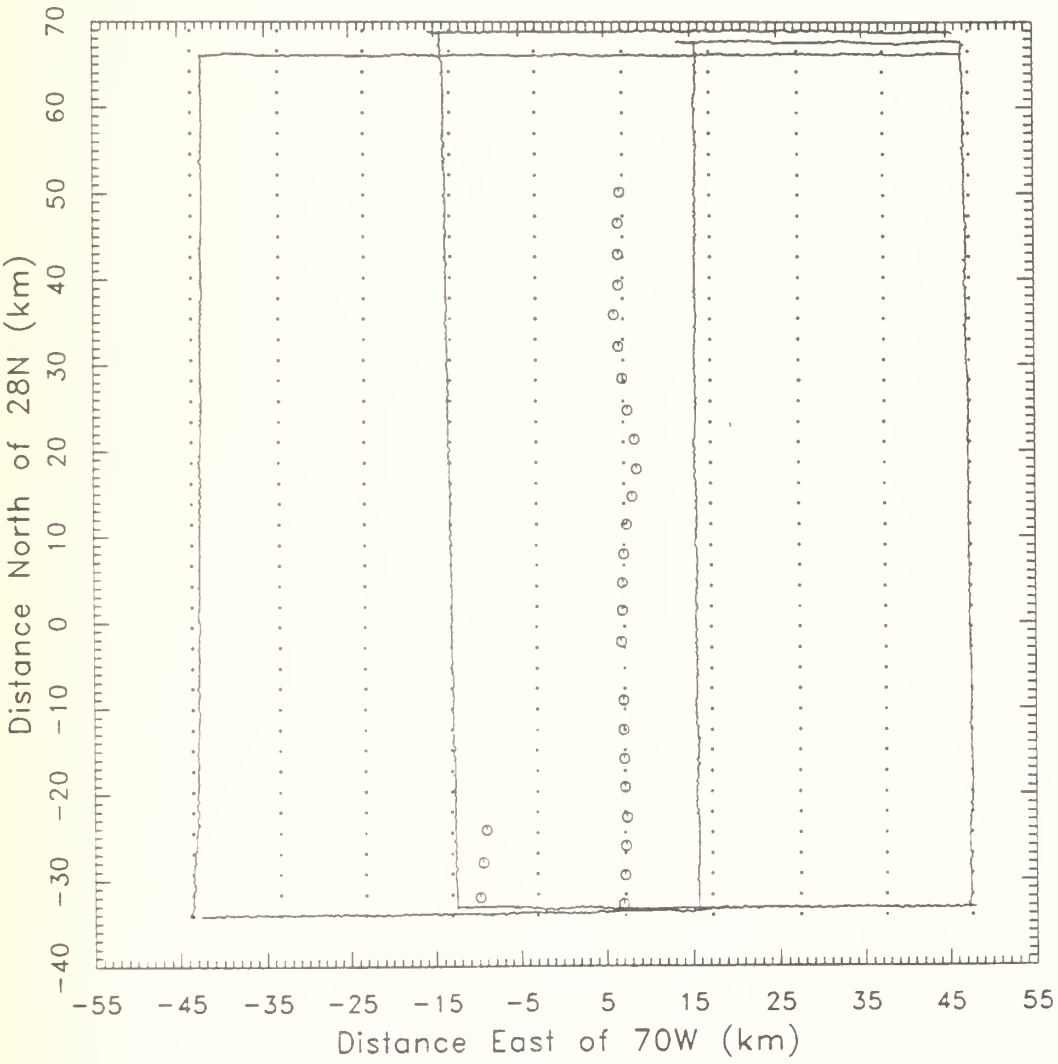

Figure C2. Flight pattern flown by NCAR Electra aircraft (--) on 17 February 1986, positions of R/V Oceanus (o) where sea surface temperature measurements were included in the analysis, and locations of regularly spaced (10 by 44) grid points (•). Distances are kilometers from reference position of 28° N, 70° W. R/V Endeavor was operating outside the flight region on this day.

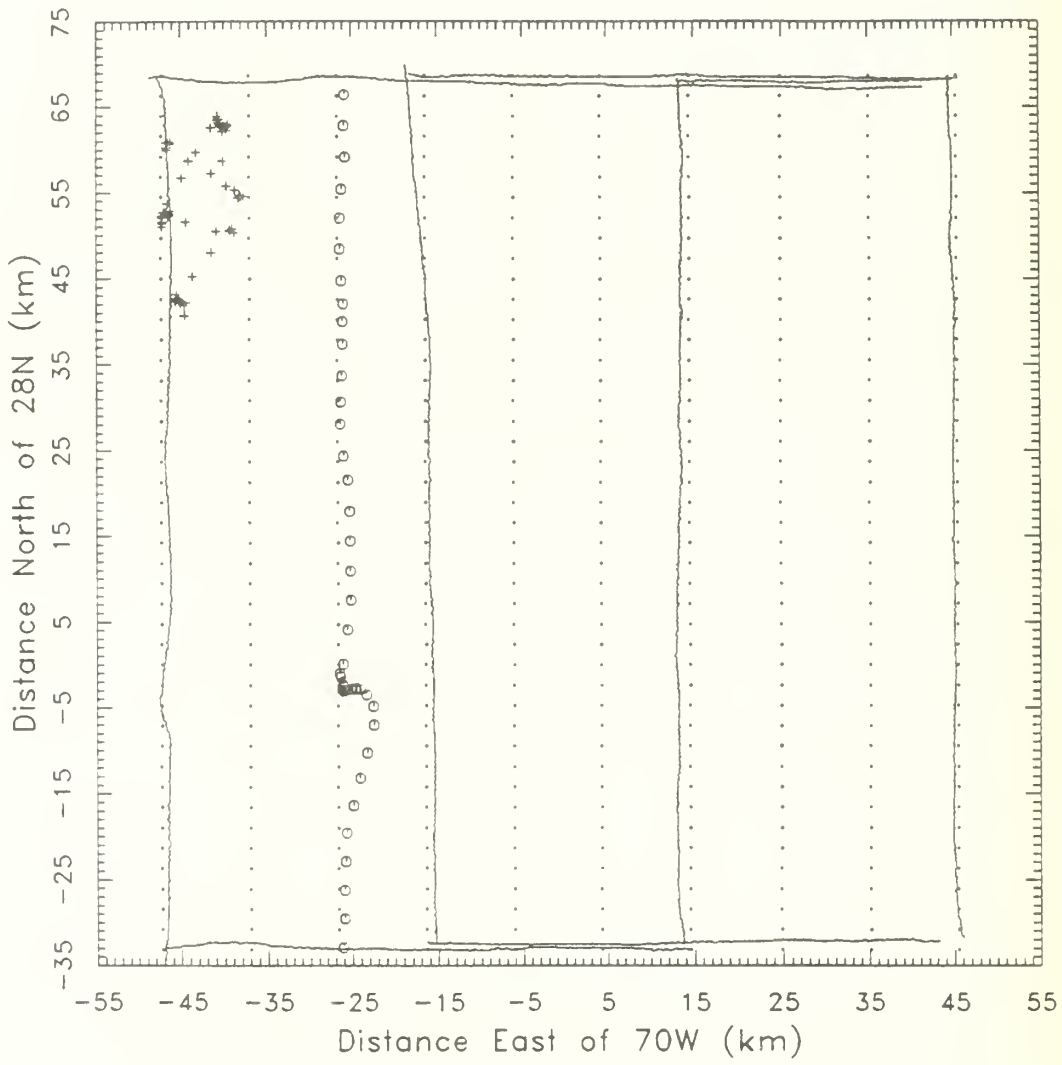

Figure C3. Flight pattern flown by NCAR Electra aircraft (--) on 18 February 1986, positions of R/V Oceanus (o) and R/V Endeavor (+) where sea surface temperature measurements were included in the analysis, and locations of regularly spaced (10 by 44) grid points (•). Distances are kilometers from reference position of 28° N, 70° W.

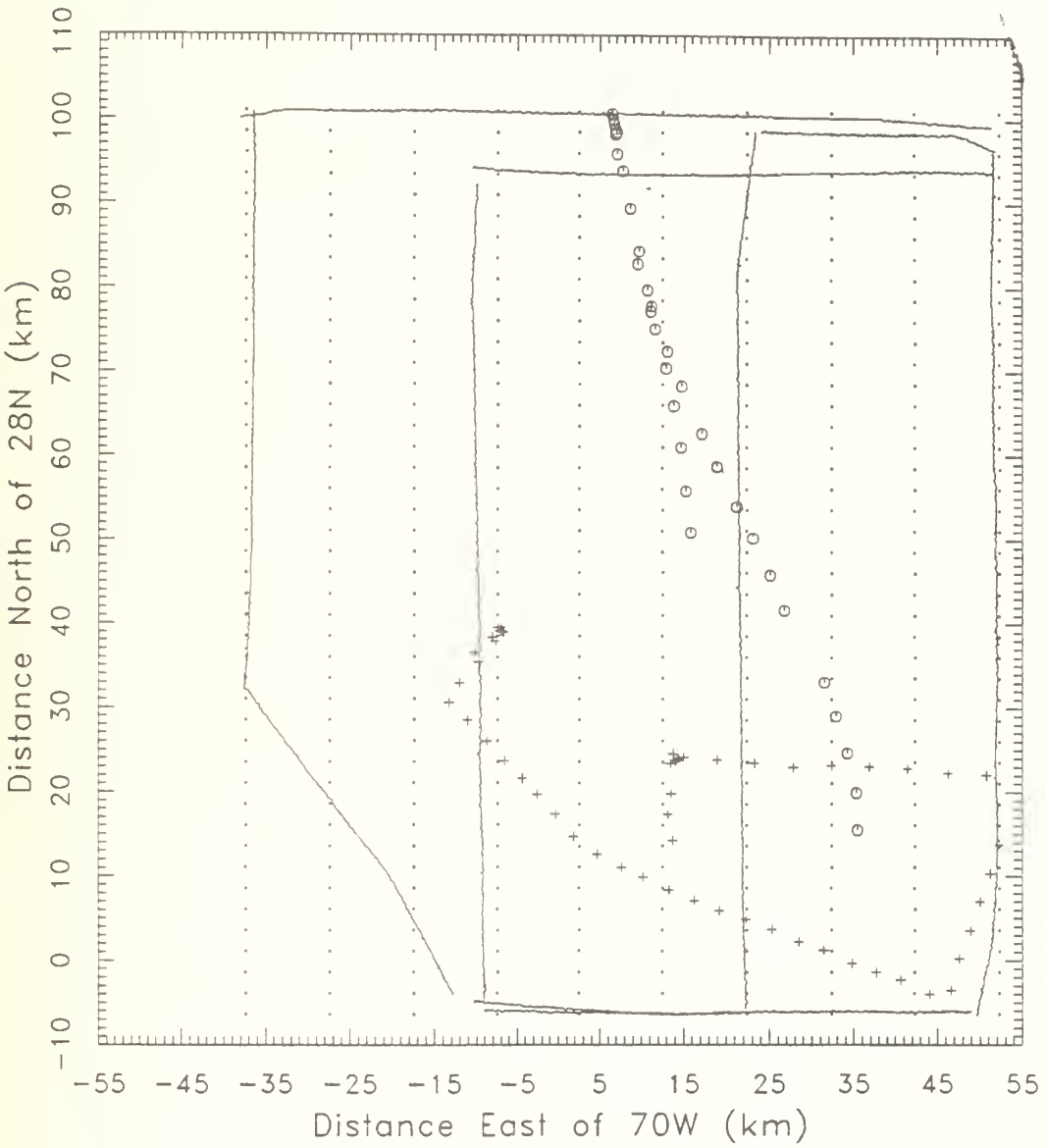

Figure C4. Flight pattern flown by NCAR Electra aircraft (--) on 21 February 1986, positions of R/V Oceanus (o) and R/V Endeavor (+) where sea surface temperature measurements were included in the analysis, and locations of regularly spaced (10 by 44) grid points (•). Distances are kilometers from reference position of 28° N, 70° W. Flight pattern in southwest corner of region was altered to avoid entering reserved air space. Diagonal leg is referred to as Leg 7b.

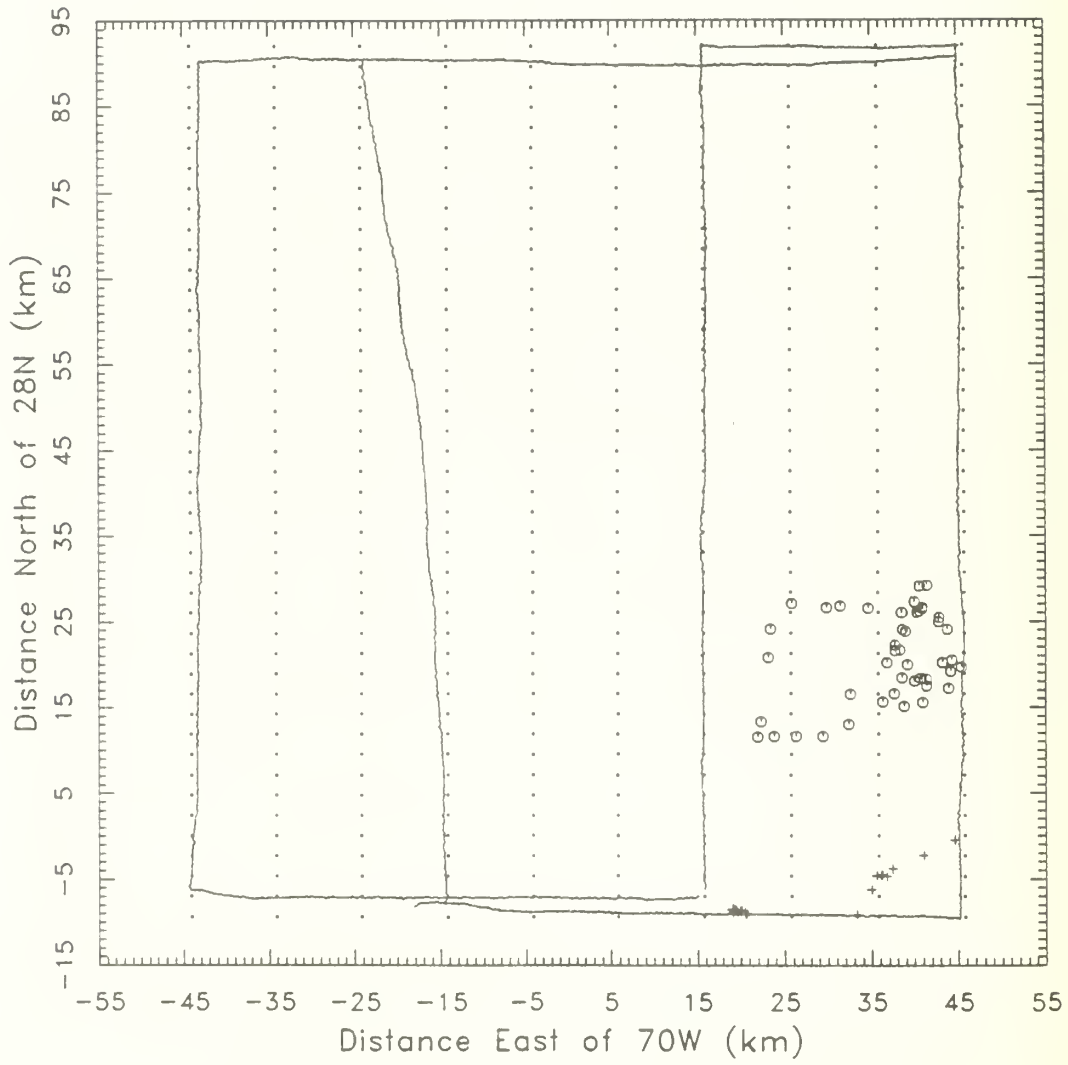

Figure C5. Flight pattern flown by NCAR Electra aircraft (--) on 24 February 1986, positions of R/V Oceanus (o) and R/V Endeavor (+) where sea surface temperature measurements were included in the analysis, and locations of regularly spaced (10 by 44) grid points (•). Distances are kilometers from reference position of 28° N, 70° W. Leg 1 was omitted from flight pattern.

D. TABLES OF REGULARLY SPACED SEA SURFACE TEMPERATURE DATA.

Table D1. Sea surface temperatures interpolated to regularly spaced grid for 16 February 1986. Grid area extends from -43.43 to 46.19 km east of 70° W (10 columns) and from -52.35 to 50.21 km north of 28° N (44 rows). Top row lists distance east of 70° W, and left column lists distance north of 28° N, for grid point locations. Temperatures are listed in degrees Celsius for each grid point.

Distance East North	-43.43	-33.47	-23.51	-13.56	-3.60	6.36	16.32	26.27	36.23	46.19
50.21	20.55	20.53	20.50	20.36	20.47	20.49	20.45	20.47	20.51	20.46
47.82	20.67	20.51	20.38	20.27	20.41	20.50	20.36	20.32	20.49	20.57
45.44	20.64	20.49	20.38	20.36	20.35	20.36	20.33	20.38	20.57	20.79
43.05	20.59	20.48	20.39	20.33	20.28	20.26	20.30	20.45	20.71	21.05
40.67	20.59	20.48	20.38	20.28	20.23	20.22	20.30	20.50	20.80	21.18
38.28	20.59	20.48	20.38	20.28	20.22	20.22	20.30	20.50	20.80	21.19
35.90	20.56	20.47	20.39	20.31	20.25	20.23	20.28	20.46	20.72	21.02
33.51	20.50	20.44	20.39	20.33	20.27	20.24	20.28	20.41	20.60	20.82
31.13	20.45	20.40	20.36	20.34	20.27	20.23	20.25	20.35	20.51	20.68
28.74	20.40	20.33	20.30	20.28	20.21	20.16	20.19	20.32	20.48	20.63
26.36	20.28	20.26	20.24	20.23	20.12	20.07	20.12	20.34	20.53	20.61
23.97	20.29	20.29	20.22	20.12	20.02	20.00	20.13	20.42	20.61	20.62
21.59	20.63	20.48	20.34	20.15	20.04	19.97	20.05	20.48	20.46	20.68
19.20	20.80	20.84	20.68	20.45	20.25	20.09	20.02	20.23	20.49	20.91
16.82	21.79	21.42	21.14	20.84	20.57	20.37	20.24	20.38	20.57	20.93
14.43	22.19	21.93	21.68	21.38	20.92	20.74	21.10	20.98	20.81	20.76
12.05	22.38	22.28	22.15	21.90	21.26	20.85	21.71	21.68	21.49	21.51
9.66	22.49	22.46	22.40	22.16	21.72	21.64	22.13	22.16	22.07	22.03
7.28	22.39	22.48	22.44	22.43	22.02	22.20	22.34	22.37	22.34	22.42
4.89	22.44	22.54	22.11	22.39	22.34	22.35	22.48	22.45	22.38	22.63
2.51	22.54	22.42	22.30	22.38	22.41	22.44	22.47	22.51	22.58	22.67
0.12	22.62	22.48	22.44	22.45	22.45	22.42	22.40	22.51	22.63	22.66
-2.26	22.62	22.55	22.51	22.49	22.44	22.39	22.39	22.49	22.61	22.70
-4.65	22.59	22.57	22.55	22.51	22.43	22.36	22.35	22.42	22.55	22.71
-7.03	22.55	22.57	22.56	22.53	22.42	22.33	22.30	22.36	22.46	22.68
-9.42	22.54	22.56	22.56	22.51	22.41	22.31	22.25	22.33	22.48	22.67
-11.80	22.58	22.57	22.55	22.49	22.39	22.30	22.27	22.35	22.48	22.68
-14.19	22.62	22.60	22.56	22.49	22.39	22.30	22.27	22.38	22.51	22.60
-16.57	22.65	22.63	22.59	22.51	22.40	22.30	22.29	22.39	22.53	22.53
-18.96	22.65	22.65	22.62	22.54	22.40	22.27	22.23	22.30	22.44	22.54
-21.34	22.63	22.66	22.66	22.60	22.40	22.20	22.08	22.14	22.33	22.61
-23.73	22.61	22.66	22.67	22.60	22.41	22.16	21.96	22.02	22.21	22.74
-26.11	22.59	22.65	22.67	22.61	22.45	22.24	22.07	22.07	22.25	22.67
-28.50	22.58	22.63	22.66	22.65	22.51	22.36	22.25	22.20	22.31	22.64
-30.88	22.57	22.61	22.62	22.60	22.53	22.44	22.37	22.31	22.32	22.59
-33.27	22.56	22.58	22.59	22.56	22.52	22.48	22.43	22.42	22.51	22.66
-35.65	22.54	22.57	22.57	22.56	22.52	22.47	22.44	22.45	22.53	22.70
-38.04	22.54	22.56	22.57	22.57	22.52	22.46	22.43	22.44	22.49	22.76
-40.42	22.52	22.55	22.57	22.57	22.52	22.45	22.43	22.47	22.60	22.76
-42.81	22.48	22.53	22.57	22.58	22.53	22.47	22.44	22.50	22.62	22.74
-45.19	22.45	22.51	22.55	22.58	22.57	22.53	22.47	22.54	22.62	22.72
-47.58	22.47	22.49	22.52	22.57	22.64	22.65	22.60	22.62	22.63	22.69
-49.96	22.39	22.46	22.52	22.57	22.68	22.75	22.62	22.69	22.70	22.70
-52.35	21.99	22.44	22.52	22.68	22.56	22.52	22.53	22.47	22.29	22.46

Table D2. Sea surface temperatures interpolated to regularly spaced grid for 17 February 1986. Grid area extends from -43.53 to 47.64 km east of 70° W (10 columns) and from -37.88 to 68.95 km north of 28° N (44 rows). Top row lists distance east of 70° W, and left column lists distance north of 28° N, for grid point locations. Temperatures are listed in degrees Celsius for each grid point.

Distance East North	-43.53	-33.40	-23.27	-13.14	-3.01	7.12	17.25	27.38	37.51	47.64
68.95	19.51	19.84	20.06	20.09	20.09	20.09	20.13	20.05	20.14	20.08
66.55	19.61	19.83	20.02	19.98	20.12	20.21	20.11	20.10	20.22	20.24
64.16	19.71	19.84	19.93	19.91	20.07	20.17	20.06	20.11	20.21	20.36
61.76	19.78	19.85	19.88	19.87	20.01	20.07	19.93	20.08	20.21	20.25
59.37	19.84	19.86	19.86	19.87	19.96	19.97	19.92	20.05	20.20	20.28
56.97	19.88	19.87	19.86	19.88	19.91	19.92	19.93	20.03	20.19	20.35
54.58	19.90	19.89	19.88	19.89	19.88	19.89	19.95	20.01	20.18	20.41
52.18	19.92	19.91	19.90	19.88	19.87	19.87	19.96	20.00	20.16	20.41
49.78	19.95	19.93	19.91	19.88	19.86	19.85	19.92	19.97	20.14	20.38
47.39	19.99	19.94	19.91	19.88	19.86	19.86	19.88	19.96	20.13	20.34
44.99	20.03	19.94	19.91	19.90	19.85	19.81	19.86	19.98	20.13	20.31
42.60	20.06	19.92	19.89	19.91	19.82	19.75	19.86	20.06	20.17	20.29
40.20	20.04	19.90	19.87	19.93	19.76	19.76	19.82	20.25	20.25	20.28
37.80	20.01	19.89	19.86	19.94	19.67	19.73	20.02	20.59	20.35	20.28
35.41	20.02	19.91	19.86	19.96	19.55	19.72	20.66	21.04	20.48	20.27
33.01	20.05	19.99	19.91	19.99	19.47	19.79	21.25	21.51	20.61	20.25
30.62	20.08	20.16	20.05	19.96	19.56	19.80	21.68	21.87	20.74	20.24
28.22	20.08	20.42	20.31	20.06	19.94	19.87	21.93	22.03	20.85	20.27
25.83	20.97	20.71	20.69	20.80	20.56	20.97	21.95	22.02	20.97	20.29
23.43	21.34	21.05	21.10	21.48	21.23	21.61	21.83	21.90	21.10	20.25
21.03	21.40	21.39	21.45	21.73	21.72	21.98	21.80	21.78	21.28	20.21
18.64	21.89	21.67	21.69	21.81	21.97	21.96	21.77	21.70	21.47	21.02
16.24	22.11	21.89	21.84	21.82	22.06	22.02	21.83	21.67	21.68	21.97
13.85	22.22	22.03	21.94	21.90	22.09	22.09	21.88	21.69	21.88	22.15
11.45	22.20	22.10	22.01	21.96	22.11	22.16	21.86	21.73	22.02	22.24
9.05	22.14	22.14	22.05	21.96	22.13	22.14	21.83	21.78	22.12	22.28
6.66	22.15	22.15	22.08	21.96	22.17	22.17	21.89	21.83	22.18	22.31
4.26	22.17	22.16	22.10	22.01	22.21	22.26	21.95	21.89	22.21	22.33
1.87	22.17	22.16	22.12	22.06	22.26	22.34	22.02	21.93	22.23	22.34
-0.53	22.17	22.16	22.14	22.13	22.30	22.34	22.06	21.98	22.24	22.32
-2.92	22.20	22.15	22.14	22.18	22.30	22.34	22.11	22.02	22.24	22.30
-5.32	22.22	22.15	22.12	22.12	22.28	22.32	22.13	22.05	22.24	22.25
-7.72	22.20	22.14	22.09	22.04	22.26	22.32	22.13	22.07	22.24	22.21
-10.11	22.17	22.14	22.07	21.99	22.24	22.36	22.12	22.09	22.24	22.20
-12.51	22.16	22.13	22.08	22.05	22.24	22.35	22.18	22.11	22.24	22.26
-14.90	22.16	22.12	22.10	22.13	22.25	22.37	22.21	22.13	22.24	22.31
-17.30	22.16	22.12	22.12	22.15	22.25	22.30	22.22	22.16	22.24	22.28
-19.70	22.13	22.11	22.13	22.15	22.25	22.24	22.23	22.16	22.23	22.23
-22.09	22.09	22.10	22.14	22.17	22.27	22.24	22.24	22.15	22.23	22.22
-24.49	22.03	22.10	22.16	22.19	22.30	22.30	22.18	22.13	22.25	22.25
-26.88	21.97	22.10	22.17	22.20	22.33	22.37	22.11	22.12	22.29	22.34
-29.28	21.97	22.11	22.18	22.20	22.35	22.35	22.08	22.17	22.35	22.43
-31.67	22.00	22.15	22.19	22.19	22.35	22.40	22.11	22.31	22.43	22.47
-34.07	22.07	22.18	22.21	22.08	22.27	22.22	22.45	22.51	22.60	22.40

Table D3. Sea surface temperatures interpolated to regularly spaced grid for 18 February 1986. Grid area extends from -47.49 to 45.49 km east of 70° W (10 columns) and from -33.16 to 68.69 km north of 28° N (44 rows). Top row lists distance east of 70° W, and left column lists distance north of 28° N, for grid point locations. Temperatures are listed in degrees Celsius for each grid point.

Distance East North	-47.29	-36.98	-26.67	-16.36	-6.05	4.25	14.56	24.87	35.18	45.49
68.69	20.57	20.04	19.88	19.92	19.94	20.02	20.01	19.92	19.89	19.95
66.32	20.60	20.02	19.65	19.83	19.96	19.87	19.89	20.00	19.99	20.03
63.95	20.39	19.96	19.57	19.79	19.97	19.80	19.87	19.98	20.04	20.09
61.58	20.02	19.83	19.55	19.80	19.96	19.81	19.89	19.97	20.03	20.07
59.22	19.93	19.72	19.54	19.83	19.96	19.83	19.93	19.99	20.02	20.03
56.85	20.17	19.75	19.49	19.79	19.97	19.84	19.96	20.00	20.02	20.04
54.48	20.53	19.75	19.40	19.77	19.99	19.80	19.90	19.97	20.02	20.08
52.11	20.50	19.66	19.24	19.81	20.01	19.75	19.84	19.93	20.02	20.10
49.74	21.22	19.56	19.24	19.87	20.03	19.71	19.80	19.92	20.04	20.15
47.37	21.41	19.58	19.25	19.85	20.04	19.68	19.79	19.92	20.08	20.24
45.00	21.48	19.76	19.25	19.82	20.04	19.68	19.79	19.95	20.15	20.40
42.64	21.57	20.03	19.02	19.79	20.03	19.71	19.85	20.03	20.23	20.45
40.27	21.52	20.29	19.35	19.78	20.02	19.79	20.00	20.17	20.34	20.50
37.90	21.60	20.52	19.31	19.78	20.00	19.87	20.13	20.36	20.54	20.64
35.53	21.79	20.74	19.79	19.80	19.99	20.02	20.32	20.64	20.87	21.03
33.16	21.72	20.98	20.31	19.75	20.02	20.27	20.72	21.07	21.29	21.44
30.79	21.71	21.21	20.46	19.70	20.13	20.63	21.27	21.54	21.67	21.79
28.42	21.71	21.41	21.03	19.78	20.33	20.99	21.68	21.89	21.93	21.91
26.06	21.93	21.55	21.21	20.39	20.59	21.26	21.77	22.01	22.05	21.99
23.69	21.98	21.65	21.31	21.11	20.90	21.51	21.84	22.03	22.09	22.08
21.32	22.00	21.73	21.48	21.48	21.21	21.70	21.90	22.05	22.11	22.12
18.95	22.02	21.79	21.48	21.60	21.47	21.83	21.98	22.08	22.14	22.18
16.58	22.04	21.85	21.68	21.76	21.66	21.90	22.03	22.11	22.17	22.23
14.21	22.06	21.91	21.87	21.74	21.79	21.92	22.02	22.11	22.20	22.28
11.84	22.07	21.96	21.97	21.84	21.87	21.93	22.01	22.13	22.23	22.33
9.47	22.08	22.00	21.92	21.88	21.93	21.97	22.06	22.16	22.26	22.37
7.11	22.09	22.03	21.85	21.89	21.97	22.01	22.12	22.20	22.29	22.38
4.74	22.13	22.05	21.95	21.87	22.00	22.02	22.13	22.22	22.30	22.38
2.37	22.14	22.05	21.97	21.85	22.04	22.03	22.13	22.23	22.31	22.37
0.00	22.10	22.05	21.97	21.88	22.08	22.05	22.15	22.24	22.30	22.36
-2.37	22.03	22.03	21.90	21.94	22.11	22.09	22.18	22.24	22.29	22.33
-4.74	21.95	22.00	21.83	21.97	22.13	22.12	22.19	22.23	22.26	22.29
-7.11	21.91	21.97	21.82	22.00	22.13	22.14	22.19	22.20	22.21	22.22
-9.47	21.89	21.95	21.84	22.04	22.12	22.13	22.16	22.16	22.14	22.11
-11.84	21.93	21.96	21.91	22.02	22.09	22.12	22.13	22.12	22.07	22.00
-14.21	21.96	21.97	22.04	22.02	22.06	22.12	22.14	22.10	22.03	21.92
-16.58	21.94	21.98	22.18	22.07	22.03	22.12	22.14	22.09	22.02	21.93
-18.95	21.91	21.99	22.22	22.09	22.02	22.10	22.09	22.07	22.04	22.00
-21.32	21.90	21.98	22.26	22.09	22.02	22.07	22.05	22.06	22.07	22.10
-23.69	21.94	21.97	22.18	22.05	22.05	22.05	22.05	22.06	22.09	22.15
-26.05	22.02	21.98	21.66	22.00	22.09	22.05	22.07	22.08	22.09	22.10
-28.42	22.10	22.03	21.71	21.98	22.14	22.07	22.09	22.12	22.11	22.06
-30.79	22.16	22.15	21.81	22.04	22.19	22.14	22.16	22.20	22.21	22.17
-33.16	22.13	22.33	21.84	22.05	22.22	22.24	22.21	22.34	22.36	22.32

Table D4. Sea surface temperatures interpolated to regularly spaced grid for 21 February 1986. Grid area extends from -37.35 to 52.33 km east of 70° W (10 columns) and from -6.36 to 100.91 km north of 28° N (44 rows). Top row lists distance east of 70° W, and left column lists distance north of 28° N, for grid point locations. Temperatures are listed in degrees Celsius for each grid point.

Distance East	-37.35	-27.39	-17.42	-7.46	2.51	12.47	22.44	32.40	42.37	52.33
North										
100.91	20.86	20.84	20.55	20.46	20.62	21.26	20.81	20.76	20.70	20.85
98.42	21.17	20.87	20.66	20.55	20.63	20.98	20.78	20.73	20.80	20.91
95.92	21.34	20.95	20.73	20.63	20.64	21.01	20.69	20.73	20.82	20.97
93.43	21.41	21.00	20.76	20.69	20.54	21.08	20.80	20.81	20.85	21.00
90.93	21.44	21.03	20.75	20.63	20.57	21.00	20.95	20.89	20.87	20.90
88.44	21.45	21.04	20.71	20.56	20.59	20.91	21.08	21.02	20.93	20.83
85.94	21.45	21.04	20.67	20.51	20.62	20.91	21.18	21.16	21.01	20.82
83.45	21.47	21.06	20.66	20.51	20.66	20.93	21.28	21.26	21.07	20.84
80.95	21.54	21.09	20.71	20.59	20.73	20.95	21.30	21.30	21.09	20.84
78.46	21.63	21.14	20.80	20.72	20.85	20.98	21.30	21.26	21.08	20.86
75.96	21.70	21.19	20.90	20.87	21.02	21.17	21.25	21.16	21.02	20.89
73.47	21.72	21.23	20.99	21.00	21.19	21.45	21.16	21.00	20.92	20.91
70.97	21.57	21.27	21.06	21.11	21.35	21.34	21.06	20.81	20.79	20.92
68.48	21.53	21.32	21.09	21.17	21.46	21.55	20.91	20.61	20.65	20.89
65.98	21.86	21.36	21.10	21.20	21.53	21.51	20.74	20.42	20.52	20.83
63.49	21.99	21.41	21.10	21.21	21.55	21.57	20.74	20.26	20.41	20.76
61.00	22.09	21.46	21.10	21.20	21.55	21.56	20.59	20.18	20.33	20.72
58.50	22.19	21.51	21.11	21.18	21.52	21.54	20.66	20.14	20.31	20.74
56.01	22.20	21.57	21.14	21.15	21.44	21.47	20.61	20.17	20.33	20.79
53.51	22.29	21.63	21.19	21.14	21.32	21.31	20.57	20.25	20.38	20.79
51.02	22.34	21.72	21.26	21.11	21.16	21.13	20.67	20.37	20.46	20.78
48.52	22.39	21.85	21.36	21.07	20.99	20.93	20.67	20.50	20.55	20.75
46.03	22.46	22.03	21.50	21.02	20.80	20.74	20.67	20.61	20.66	20.73
43.53	22.51	22.25	21.72	20.99	20.63	20.58	20.67	20.69	20.79	20.74
41.04	22.56	22.51	22.06	21.07	20.47	20.46	20.62	20.71	20.91	21.24
38.54	22.56	22.75	22.49	21.12	20.36	20.39	20.60	20.70	21.01	21.81
36.05	22.50	22.94	22.87	21.10	20.35	20.37	20.61	20.66	21.12	22.09
33.55	22.51	23.05	22.95	21.46	20.47	20.40	20.53	20.59	21.25	22.36
31.06	22.54	23.05	23.04	21.74	20.67	20.49	20.54	20.51	21.52	22.46
28.57	22.58	22.96	23.08	21.98	20.95	20.62	20.62	20.59	22.01	22.69
26.07	22.64	22.84	22.87	22.09	21.36	20.72	21.28	21.46	22.65	22.85
23.58	22.75	22.74	22.60	22.30	21.90	20.85	21.83	21.98	23.13	22.88
21.08	22.85	22.66	22.44	22.41	22.41	21.33	22.11	22.25	22.77	23.43
18.59	22.95	22.65	22.46	22.59	22.61	21.73	22.41	22.40	22.59	22.91
16.09	23.03	22.80	22.60	22.53	22.68	22.15	22.48	22.55	22.62	22.90
13.60	23.13	22.98	22.78	22.66	22.81	22.37	22.75	22.74	22.76	23.10
11.10	23.24	23.11	22.90	22.78	22.83	22.67	22.90	22.94	22.95	23.25
8.61	23.35	23.18	22.95	22.84	22.87	23.13	22.86	23.15	23.13	22.84
6.11	23.45	23.24	22.97	22.84	22.89	23.11	23.32	23.33	23.25	22.98
3.62	23.53	23.29	23.02	22.81	22.87	23.00	22.97	23.41	23.31	22.98
1.12	23.59	23.33	23.09	22.78	22.83	22.90	22.94	23.26	23.29	22.90
-1.37	23.64	23.36	23.10	22.76	22.82	22.87	22.91	22.98	23.23	22.87
-3.87	23.53	23.37	23.08	22.94	22.84	22.88	22.90	22.95	23.29	22.82
-6.36	23.55	23.38	23.05	22.81	22.91	22.91	22.91	22.94	22.82	22.82

Table D5. Sea surface temperatures interpolated to regularly spaced grid for 24 February 1986. Grid area extends from -44.14 to 45.79 km east of 70° W (10 columns) and from -9.36 to 92.01 km north of 28° N (44 rows). Top row lists distance east of 70° W, and left column lists distance north of 28° N, for grid point locations. Temperatures are listed in degrees Celsius for each grid point.

Distance East North	-44.14	-34.15	-24.16	-14.16	-4.17	5.82	15.81	25.81	35.80	45.79
92.01	22.14	21.07	20.72	21.23	21.43	21.51	21.25	20.06	20.03	20.59
89.65	21.99	21.50	20.84	21.38	21.40	21.43	21.41	20.42	20.50	20.75
87.30	21.84	21.55	21.14	21.40	21.41	21.43	21.42	20.91	20.85	20.99
84.94	21.82	21.64	21.26	21.44	21.42	21.41	21.41	21.18	21.08	21.07
82.58	21.86	21.76	21.73	21.50	21.43	21.37	21.31	21.30	21.25	21.15
80.22	21.96	21.87	21.79	21.57	21.44	21.34	21.23	21.36	21.36	21.23
77.87	22.09	21.95	21.80	21.60	21.45	21.35	21.30	21.40	21.42	21.31
75.51	22.21	22.00	21.79	21.59	21.45	21.37	21.39	21.44	21.46	21.41
73.15	22.26	22.03	21.79	21.58	21.44	21.39	21.42	21.46	21.49	21.52
70.79	22.28	22.05	21.79	21.57	21.42	21.39	21.42	21.45	21.49	21.60
68.44	22.33	22.07	21.81	21.57	21.38	21.35	21.41	21.40	21.47	21.66
66.08	22.37	22.08	21.82	21.56	21.34	21.25	21.35	21.29	21.43	21.71
63.72	22.35	22.10	21.84	21.57	21.31	21.11	21.11	21.14	21.39	21.75
61.36	22.31	22.12	21.88	21.61	21.29	20.96	20.76	20.97	21.36	21.78
59.01	22.27	22.13	21.94	21.67	21.31	20.87	20.52	20.88	21.35	21.79
56.65	22.26	22.14	21.99	21.73	21.36	20.91	20.52	20.90	21.36	21.79
54.29	22.25	22.15	22.02	21.78	21.43	21.07	20.88	21.04	21.40	21.80
51.93	22.24	22.17	22.04	21.81	21.53	21.29	21.23	21.25	21.47	21.79
49.58	22.23	22.17	22.06	21.86	21.63	21.51	21.54	21.45	21.53	21.78
47.22	22.26	22.18	22.07	21.90	21.73	21.68	21.76	21.60	21.60	21.74
44.86	22.30	22.18	22.07	21.94	21.81	21.78	21.76	21.69	21.64	21.66
42.50	22.31	22.18	22.05	21.94	21.88	21.84	21.77	21.74	21.67	21.57
40.15	22.32	22.18	22.02	21.93	21.92	21.90	21.81	21.79	21.68	21.50
37.79	22.38	22.16	21.99	21.92	21.94	21.95	21.91	21.84	21.69	21.47
35.43	22.41	22.13	21.98	21.92	21.96	21.99	22.02	21.89	21.71	21.45
33.07	22.36	22.09	21.98	21.94	21.97	22.03	22.05	21.96	21.73	21.42
30.72	22.12	22.05	21.98	21.97	21.98	22.04	22.08	22.04	21.76	21.35
28.36	21.90	22.00	21.98	21.95	21.98	22.05	22.14	22.15	21.78	21.24
26.00	21.91	21.97	21.97	21.94	21.98	22.05	22.17	22.30	21.79	21.08
23.64	21.97	21.96	21.97	21.96	21.98	22.05	22.20	22.33	21.89	20.84
21.29	21.97	21.96	21.98	21.99	21.97	22.04	22.26	22.40	21.78	20.61
18.93	21.96	21.98	21.98	21.97	21.97	22.03	22.25	22.53	21.54	20.40
16.57	21.97	21.99	21.98	21.96	21.96	22.02	22.22	22.63	21.11	20.67
14.21	22.08	22.01	21.97	21.95	21.94	22.01	22.19	22.43	21.76	20.85
11.86	22.18	22.01	21.95	21.94	21.93	21.99	22.22	22.34	22.02	21.54
9.50	22.17	22.00	21.92	21.91	21.92	21.98	22.11	22.25	22.13	22.09
7.14	22.12	21.99	21.89	21.87	21.91	21.99	22.12	22.20	22.19	22.28
4.78	22.12	21.97	21.87	21.85	21.90	22.01	22.14	22.19	22.23	22.27
2.43	22.11	21.96	21.87	21.84	21.91	22.03	22.13	22.18	22.24	22.21
0.07	22.08	22.00	21.89	21.87	21.94	22.07	22.13	22.18	22.24	22.22
-2.29	22.07	22.08	21.94	21.88	22.01	22.11	22.14	22.18	22.24	22.25
-4.65	22.15	22.21	22.05	21.78	22.11	22.16	22.15	22.19	22.24	22.29
-7.00	22.41	22.36	22.20	22.17	22.21	22.19	22.20	22.24	22.21	22.33
-9.36	22.68	22.54	22.40	22.29	22.28	22.23	22.20	22.34	22.14	22.39

E. CONTOURS OF SEA SURFACE TEMPERATURE.

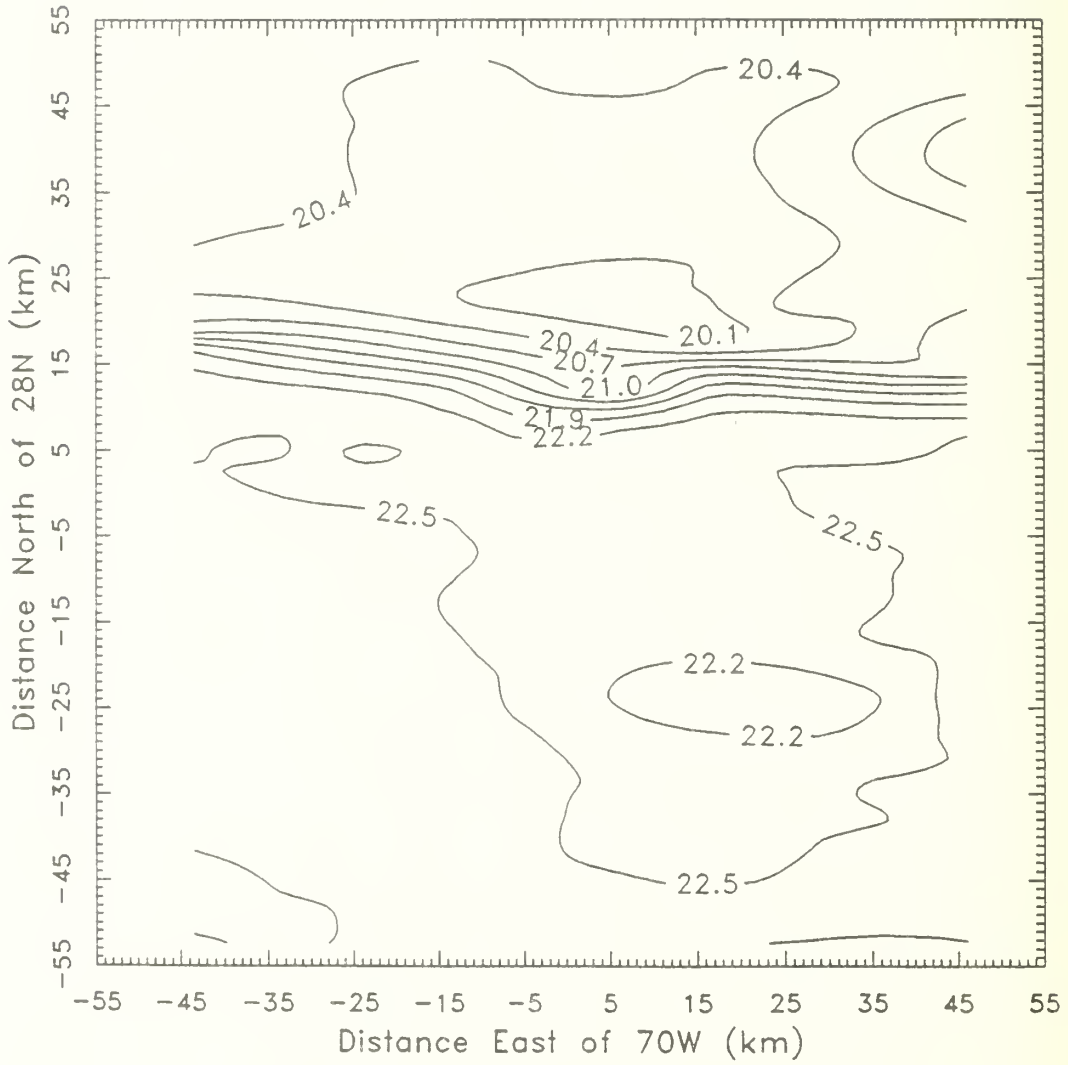

Figure E1. Contours of sea surface temperature over NCAR Electra flight region for 16 February 1986. Ocean front is aligned primarily east-west and lies in a region 10-20 km north of reference latitude, 28° N. Contour interval is 0.3° C.

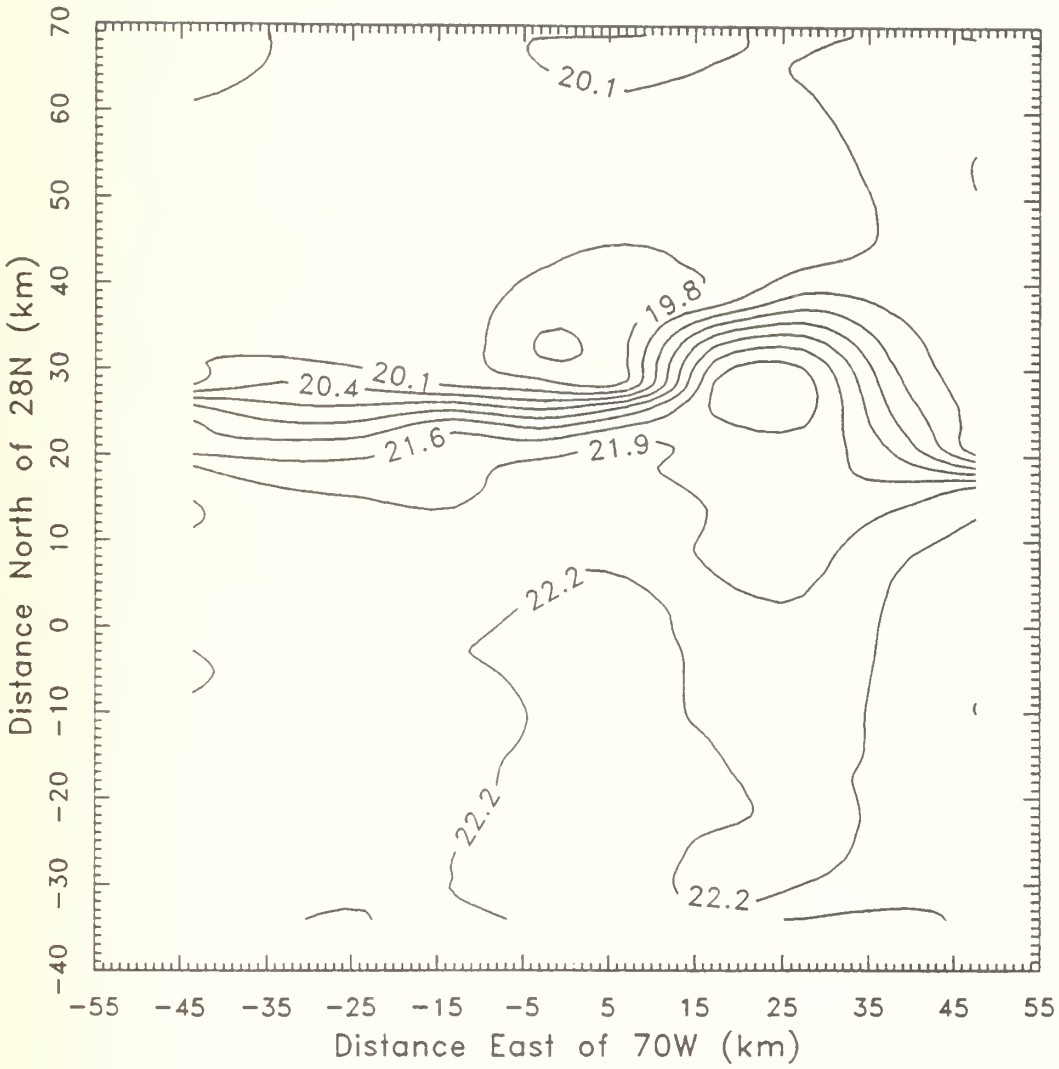

Figure E2. Contours of sea surface temperature over NCAR Electra flight region for 17 February 1986. Ocean front is aligned primarily east-west with a tongue of warm water extending northward between 10 and 40 km east of reference longitude, 70° W. Western portion of frontal region has moved ~5 km south since 16 February. Contour interval is 0.3° C.

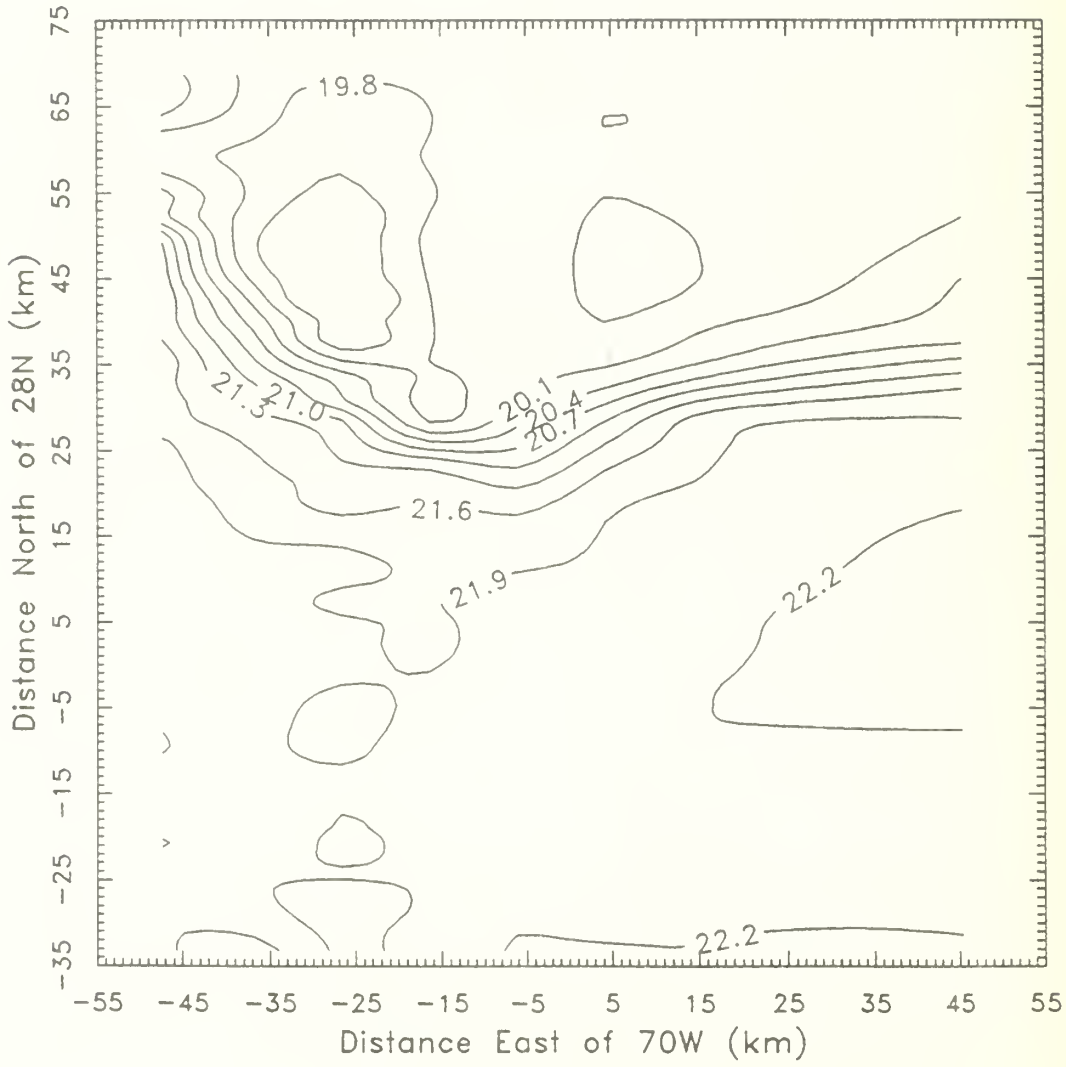

Figure E3. Contours of sea surface temperature over NCAR Electra flight region for 18 February 1986. Character of SST field has changed dramatically since the previous day, with much warmer surface water in the western portion of region. The ocean front has deformed considerably. Contour interval is 0.3° C.

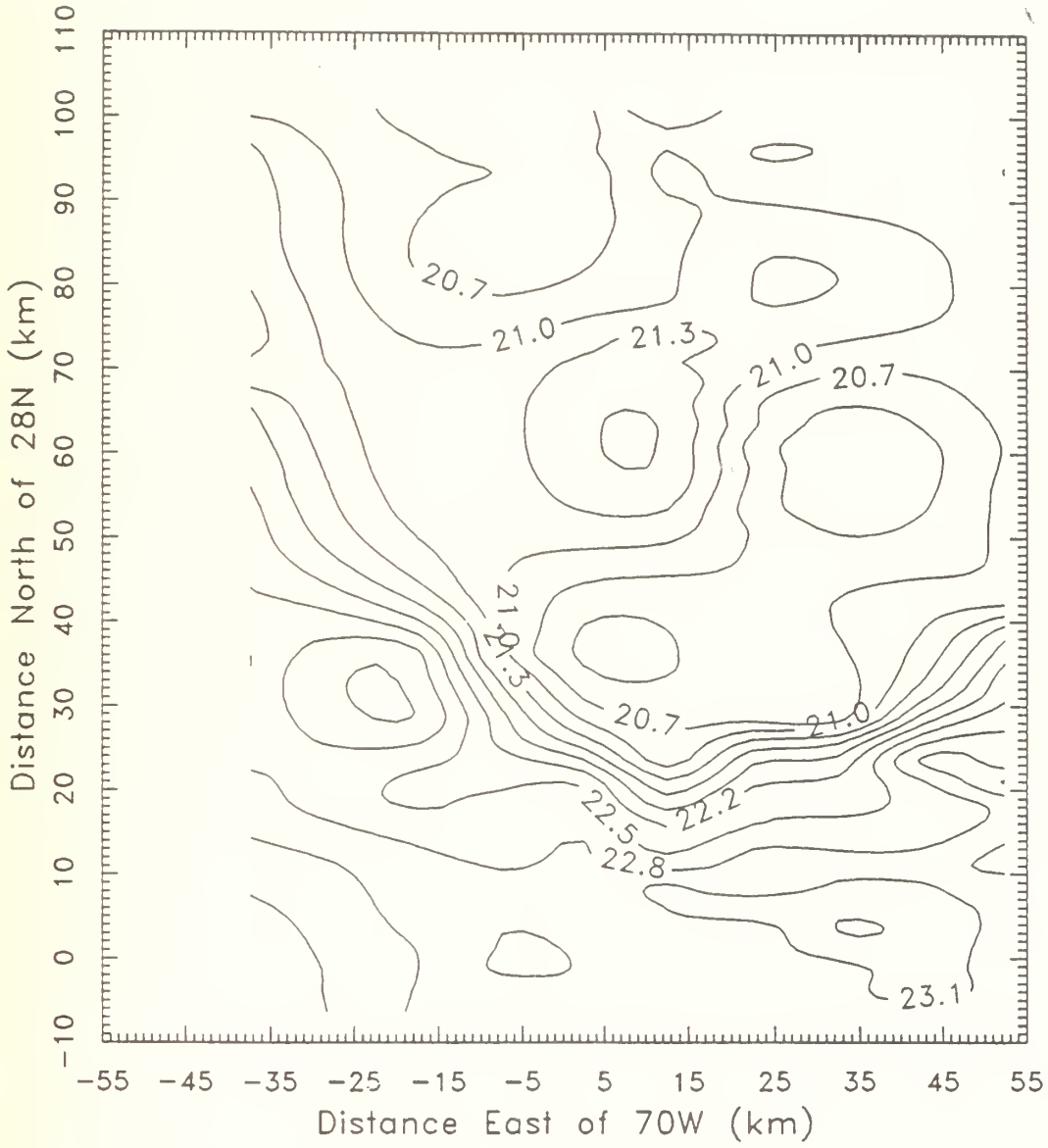

Figure E4. Contours of sea surface temperature over NCAR Electra flight region for 21 February 1986. The strongest portion of the ocean front is in SE portion of the region. A "ridge" of warmer water extends NE from the center of the flight area. Contour interval is 0.3° C.

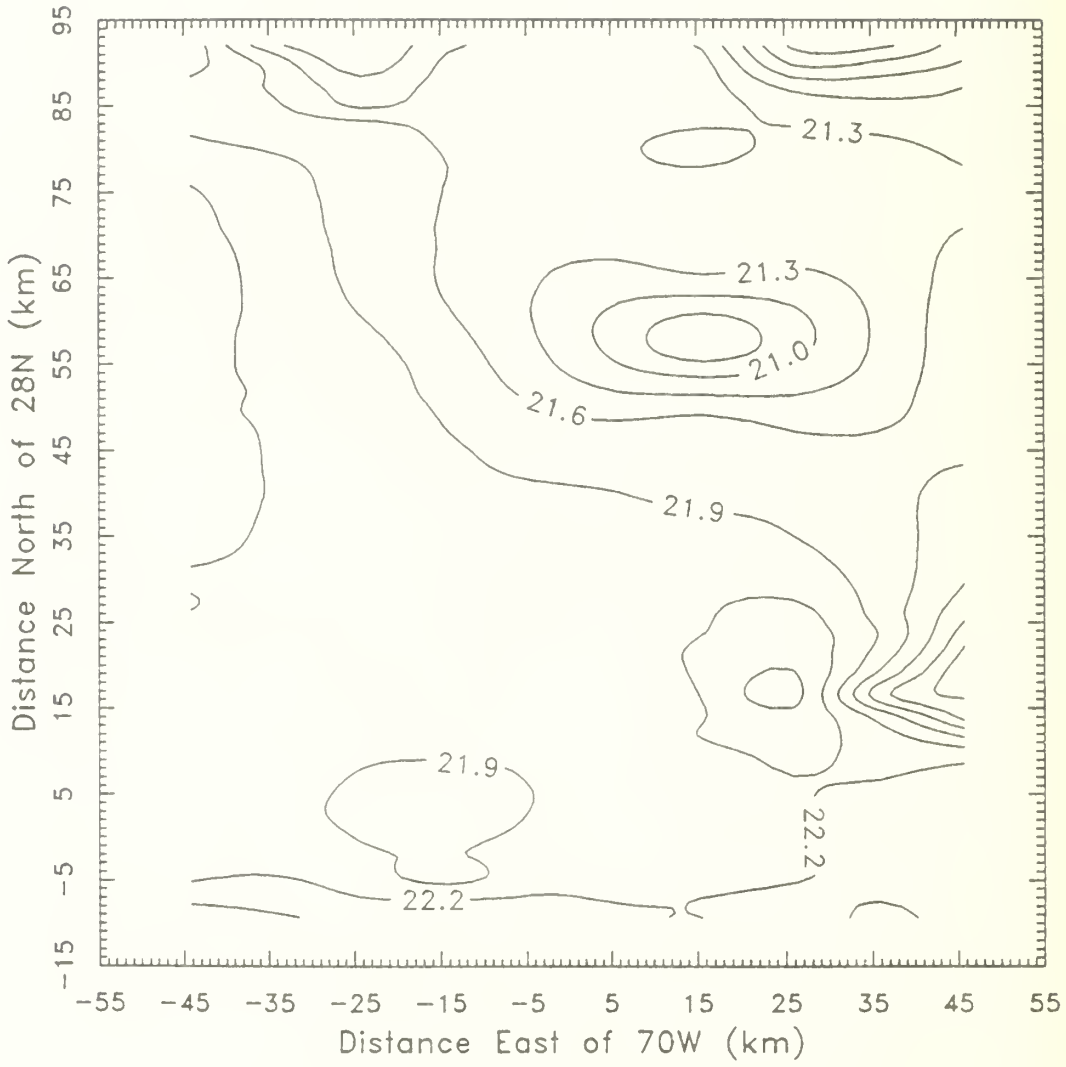

Figure E5. Contours of sea surface temperature over NCAR Electra flight region for 24 February 1986. Ocean front is not well defined. Two distinct cool pockets remain within the flight region. Contour interval is 0.3° C.

Distribution List

	No. of Copies
Dr. Robert F. Abbey Office of Naval Research 800 North Quincy Street Arlington, VA 22217	1
Dr. Joost Businger NCAR P.O. Box 3000 Boulder, CO 80307	1
Dr. Kenneth Davidson (Code 63Ds) Department of Meteorology Naval Postgraduate School Monterey, CA 93943-5000	2
Dr. Carl Friehe Mechanical Engineering University of California, Irvine Irvine, CA 92717	2
Dr. Gary K. Greenhut NOAA/ERL/ R/E2 325 Broadway Boulder, CO 80303	1
Dr. Howard Hanson CIRES P. O. Box 449 Boulder, CO 80309	1
Dr. Warren Johnson NCAR P. O. Box 3000 Boulder, CO 80307	1
Dr. Siri Jodha Singh Khalsa CIRES P. O. Box 449 Boulder, CO 80309	1
Dr. Bill Large Department of Meteorology University of British Columbia Vancouver, B.C., CANADA	1
Dr. Don Lenschow NCAR P. O. Box 3000 Boulder, CO 80307	1

Dr. F. K. Li Jet Propulsion Laboratory MS 183-701 4800 Oak Grove Drive Pasadena, CA 91109	1
Dr. William Plant Woods Hole Oceanographic Institution Woods Hole, MA 02543	1
Dr. Robert J. Renard (Code 63Rd) Department of Meteorology Naval Postgraduate School Monterey, CA 93943-5000	1
Dr. William J. Shaw (Code 63Sr) Department of Meteorology Naval Postgraduate School Monterey, CA 93943-5000	212
Dr. Steve Stage Department of Meteorology Florida State University Tallahassee, FL 32301	2
Dr. Robert A. Weller Woods Hole Oceanographic Institution Woods Hole, MA 02543	1
Library (Code 0142) Naval Postgraduate School Monterey, CA 93943-5000	2
Research Administration (Code 012) Naval Postgraduate School Monterey, CA 93943-5000	1
Defense Technical Information Center Cameron Station Alexandria, VA 22304-6145	2
National Science Foundation Washington, DC 20440	1

DUDLEY KNOX LIBRARY
3 2768 00342624 8